

**MACHINE LEARNING-DRIVEN OPTIMIZATION OF UAV  
AERODYNAMICS USING CFD SIMULATIONS FOR ENHANCED  
PERFORMANCE**



by

Qurrat-Ul-Hussnain

Emaan Noor

Supervisor:

Dr Muhammad Umer Sohail

Department of Aeronautics and Astronautics

Institute of Space Technology, Islamabad

**MACHINE LEARNING-DRIVEN OPTIMIZATION OF UAV  
AERODYNAMICS USING CFD SIMULATIONS FOR ENHANCED  
PERFORMANCE**

A thesis submitted to the  
  
Institute of Space Technology in  
  
partial fulfillment of the requirements  
  
for the degree of Bachelor of Science in  
  
Aerospace Engineering.

by

Qurrat-Ul-Hussnain

Emaan Noor

Supervisor:

Dr Muhammad Umer Sohail

Department of Aeronautics and Astronautics

Institute of Space Technology, Islamabad 2025

Institute of Space Technology

Department of Aeronautics & Astronautics



**MACHINE LEARNING-DRIVEN OPTIMIZATION OF UAV  
AERODYNAMICS USING CFD SIMULATIONS FOR ENHANCED  
PERFORMANCE**

by

Qurrat-Ul-Hussnain

Emaan Noor

APPROVAL BY SUPERVISOR

---

## **SUPERVISOR'S DECLARATION**

This is to certify that the research work described in this thesis is the original work of author(s) and has been carried out under my direct supervision. I have personally gone through all the data/results/materials reported in the manuscript and certify their correctness/authenticity. I further certify that the material included in this thesis is not plagiarized and has not been used in part or fully in a manuscript already submitted or in the process of submission in partial/complete fulfillment of the award of any other degree from any institution. I also certify that the thesis has been prepared under my supervision according to the prescribed format and I endorse its evaluation for the award of Bachelor of Science in Aerospace Engineering degree through the official procedures of the institute.

---

Dr Muhammad Umer Sohail

## **AUTHORS' DECLARATION**

We take full responsibility of the research work conducted during BS Thesis titled “MACHINE LEARNING-DRIVEN UAV AERODYNAMICS AND PERFORMANCE OPTIMIZATION LEVERAGING ENHANCED CFD”. We solemnly declare that the research and development work presented in this Thesis is done solely by us with no significant help from any other person; however, small help wherever taken is duly acknowledged. We have also written the complete thesis by ourselves. Moreover, we have not presented this thesis (or substantially similar research and development work) or any part of the thesis to any other degree awarding institution within Pakistan or abroad. We understand the management of IST has zero tolerance policy towards plagiarism. Therefore, we as the author of the abovementioned thesis, solemnly declare that no portion of our thesis has been plagiarized and any material used in the thesis from other sources is properly referenced. Moreover, the thesis does not contain any literal citing (verbatim) of more than 70 words (total) even by giving a reference unless we have obtained the written permission of the publisher to do so. Furthermore, the work presented in the thesis is our own original work and we have positively cited the related work of the other researchers by clearly differentiating our work from their relevant work. We further understand that if we are found guilty of any form of plagiarism in our thesis work even after my graduation, the Institute reserves the right to revoke our BS degree. Moreover, the Institute will also have the right to publish our name on its website that keeps a record of the students who plagiarized in their thesis work.

---

Qurrat-Ul-Hussnain

210101018

---

Emaan Noor

210101076

We hereby acknowledge that submitted thesis/report paper is the final version and should be scrutinized for plagiarism as per IST policy.

---

Dr Muhammad Umer Sohail

Dated: \_\_\_\_\_

---

Verified by Plagiarism Cell Officer

Dated: \_\_\_\_\_

Copyright © 2025 This document is jointly copyrighted by the author and the Institute of Space Technology (IST). Both the author and IST can use, publish or reproduce this document in any form. Under the copyright law no part of this document can be reproduced by anyone, except copyright holders, without the permission of the author.

## **Abstract**

In this thesis, the power of Machine Learning (ML) and Computational Fluid Dynamics (CFD) is combined to create an intelligent aerodynamic prediction and optimization tool for Unmanned Aerial Vehicles (UAVs). Ten NACA airfoils are compared in 2D and 3D CFD analysis at subsonic Mach numbers (0.02–0.3) and angles of attack ( $-2^{\circ}$ – $10^{\circ}$ ) to start the study. To guarantee precision and consistency, the aerodynamic coefficients ( $C_L$  and  $C_D$ ) were verified.

To precisely predict lift and drag coefficients, a machine learning model was trained on a dataset of more than 28,000 CFD data using a Python-based gradient optimization framework. Rapid aerodynamic estimation for both 2D airfoils and 3D wing geometries using techniques like the Vortex Lattice Method (VLM) and turbulent models was made possible by the model's further integration into an interactive Streamlit-based interface. The resultant tool offers immediate, accurate predictions appropriate for conceptual design stages, greatly cutting down on the time and computational expense related to UAV aerodynamic design. The system is applicable to defense, commercial, and research applications because it is open-ended and has the potential to expand into multiple flight regimes beyond cruise-condition analysis.



## Table of Contents

APPROVAL BY SUPERVISOR.....	iii
SUPERVISOR’S DECLARATION.....	iv
AUTHORS’ DECLARATION.....	v
Copyright © 2025 .....	vii
Abstract .....	viii
Table of Contents .....	ix
List Of Figures .....	xiv
List of Tables.....	xvii
1. Introduction.....	1
1.1 UAVs in modern aerospace systems .....	1
1.2 Importance of Aerodynamic Efficiency for MALE UAVs .....	2
1.3 Objectives of the Project.....	4
1.4 Scope.....	4
1.5 Limitations .....	5
2. Literature Review.....	6
2.1 Studies on CFD-Based UAV Optimization.....	6
2.2 Applications for Machine Learning in Aerodynamics .....	6
2.3 Summary of Gaps in Current Research .....	7
3. Airfoil Selection .....	8

3.1	Airfoil Selection and Geometry Creation .....	8
3.2	Focus on Cruise Efficiency in Airfoil Evaluation .....	9
4.	Parameters for 2D and 3D Dataset Collection .....	11
4.1	2D Analysis Parameters: .....	11
4.2	3D Analysis Parameters .....	11
4.3	CFD-Based Airfoil Analysis .....	12
4.4	CFD-Based Wing Analysis .....	13
4.5	Constraints of our project.....	13
4.6	Reason for Limitations.....	14
5.	Simulation Tools and their working.....	15
5.1	XFLR5 Approach.....	15
5.1.1	2D Analysis:.....	15
5.1.2	3D Analysis:.....	16
5.2	Ansys Approach .....	16
	Meshing Software .....	18
5.2.1	Mesh Type:.....	19
5.3	Parametric Method:.....	20
6.	Validation of Results and Data Extraction .....	22
6.1.1	Experimental Data Comparison:.....	22
6.1.2	NACA 4412 Validation: .....	22

6.1.3	NACA 0012 Validation .....	23
6.2	Data Collection: .....	24
6.2.1	2D Dataset.....	24
6.2.2	3D Dataset.....	25
6.3	Data Conversion: .....	26
7.	Predicting Machine Learning Model .....	27
7.1	Multiple Regression .....	28
7.2	Gradient-Based Optimization .....	30
8.	Performance optimizer for UAVs .....	32
8.1	Objective Function:.....	32
8.1.1	Optimizing Range of UAVs .....	32
8.1.2	Drag Model (Raymer’s approach): .....	32
8.1	3 Optimizing endurance of UAVs.....	32
8.2	Design Variables: .....	33
8.2.1	Constraints: .....	33
8.3	Output of Code:.....	33
8.4	Conclusion: .....	34
9.	Machine learning model training.....	35
9.1	Regression Algorithms applied:.....	35
9.1.1	Random forest:.....	35

9.1.2	Multiple linear regression: .....	35
9.1.3	XG – boost Regressor .....	36
9.1.4	Support Vector Regressor: .....	36
9.2	For 3D Dataset: .....	37
9.2.1	Random forest:.....	37
9.2.2	Gradient boost:.....	38
9.3	Conclusion: .....	38
10.	User Interface Development .....	41
10.1	Development Environment .....	41
10.2	Frontend .....	42
10.3	Backend.....	42
10.4	System Architecture .....	42
10.5	UAV OPTIMIZER SUITE:.....	44
	.....	44
10.6	3D Aerodynamic Prediction Tool: .....	46
11.	Future Goals and Industrial Relevance .....	48
11.1	Rapid UAV Design Prototyping.....	48
11.2	Integration into UAV Design Software .....	48
11.3	Customized UAV Performance Optimization .....	48
12.	Sustainable Development Goals: .....	49

12.1 Goal 9:.....	49
12.2 Goal 12.....	49
13.References:.....	50

## List Of Figures

Figure 1.1 Gantt Chart .....	5
Figure 3. 1 Comparison of L/D Max and L/D Cruise for selected NACA Airfoils.....	10
Figure 4.1 Cases for 2D Analysis of Airfoil .....	12
Figure 4. 2 Cases for 3D Analysis of Wings .....	13
Figure 5. 1 2D Airfoil Analysis in XFLR5.....	15
Figure 5. 2 3D Wing Analysis in XFLR5 .....	16
Figure 5. 3 2D Domain .....	18
Figure 5. 4 3D Geometry in Ansys .....	18
Figure 5. 5 Mesh at the boundary of the airfoil .....	19
Figure 5. 6 Mesh Quality.....	19
Figure 5. 7 mesh refinement.....	20
Figure 5. 8 Mesh Skewness Study.....	20
Figure 5. 9 Parametric approach in Ansys .....	21
Figure 6. 1 MATLAB Graph validated- Naca 4412.....	23
Figure 6. 2 Paper graph of naca 4412 .....	23
Figure 6. 3 Paper Graph of naca 0012.....	23
Figure 6. 4 MATLAB Graph of Naca 0012-Validated .....	23
Figure 6. 5 2D Dataset (1) .....	24

Figure 6. 6 2D Dataset (2) .....	25
Figure 6. 7 3D Dataset (1) .....	25
Figure 6. 8 3D Dataset (2) .....	26
Figure 7. 1 Regression overview.....	27
Figure 7. 2 Multiple regression generated graph.....	29
Figure 7. 3 Gradient Based Optimizer .....	30
Figure 7. 4 Generic flowchart of gradient based optimizer .....	31
Figure 8. 1 Flowchart of working of Performance optimizer .....	33
Figure 8. 2 Optimized L/D Range and Endurance .....	33
Figure 9. 1 Random Forest for 2D Dataset .....	35
Figure 9. 2 Multiple regression for 2DDataset .....	36
Figure 9. 3 XG-Boost regressor for 2D Dataset.....	36
Figure 9. 4 Support vector regressor for 2D Dataset.....	37
Figure 9. 5 Random Forest for 3D Dataset .....	37
Figure 9. 6 Gradient boost for 3D Dataset .....	38
Figure 9. 7 A comparison of different models with their $R^2$ .....	39
Figure 9. 8 XG Boost Regression Graph for 2D-CD .....	40
Figure 9. 9 XG-Boost regression for 2D-Cl .....	40

Figure 9. 10 Random Forest for 3D -CD .....	41
Figure 9. 11 Random Forest 3D Dataset-CL .....	41
Figure 10. 1 Options of Airfoil in interface.....	43
Figure 10. 2 Input parameters in 2D Interface .....	43
Figure 10. 3 2D Aero Analysis interface with predicted CL and CD .....	43
Figure 10. 4 Optimizer interface7 .....	44
Figure 10. 5 Optimized performance parameters .....	44
Figure 10. 6 Optimized results in form of graphs.....	45
Figure 10. 7 3D interface parameters (flow) .....	46
Figure 10. 8 3D Input parameters.....	46
Figure 10. 9 Results display-3D Cl and Cd prediction .....	46
Figure 10. 10 Input summery in Interface .....	47



## List of Tables

Table 2. 1 Naca Airfoils that are selected based on literature review .....	8
Table 4. 1 Limitations of our simulation tool .....	13
Table 7. 1 Diff b/w Classification and Regression.....	28
Table 7. 2 Types of Optimizers .....	29

# **1. Introduction**

## **1.1 UAVs in modern aerospace systems**

In technical terms, drones are known as unmanned aerial systems (UAS) or unmanned aerial vehicles (UAVs). These are remotely or autonomously piloted aircraft that can be controlled from the ground and fly without a human pilot on board. Wireless communication beyond human trajectory frequently necessitates the use of UAVs. Military operations, mining, agriculture, and general-purpose uses like surveillance, exploration, rescue, delivery of weapons and products, mapping and surveying, entertainment, photography, etc. are just a few of the many uses for drones that have emerged recently.

A variety of Micro-electromechanical Systems (MEMS), such as sensors, cameras, controllers, and more, are installed on these UAVs. UAVs support implicit particularities like access to disaster-stricken areas, quick mobility, airborne missions, and payload features. This manuscript reviews a novel taxonomy of flying drones with their explicitly defined applications, encompassing UAVs to smart sensors.

Despite these alluring advantages, UAVs are limited in their ability to operate due to several serious issues, including limited payload carrying capacity, flight autonomy, path planning, battery endurance, and flight time. It is generally not advised to load heavy objects, like batteries. Therefore, the main objective of this study is to shed light on the potential of UAVs as well as their features and functional problems. A thorough analysis of UAV types, swarms, classifications, charging techniques, and regulations is given in this study.

## **1.2 Importance of Aerodynamic Efficiency for MALE UAVs**

Medium Altitude Long Endurance (MALE) UAVs are built to function for extended periods of time, frequently longer than 24 hours, at altitudes between 10,000 and 30,000 feet. These UAVs are essential for environmental monitoring, disaster relief, border surveillance, and military reconnaissance. Aerodynamic efficiency is critical in such long-duration missions. Range and loiter time are directly improved by a higher lift-to-drag ratio, which allows the UAV to use less fuel or power while keeping altitude and stability. Effective aerodynamic design also lessens the structural load on the airframe and increases payload capacity. Optimizing aerodynamic performance is crucial to mission success for MALE UAVs, where endurance and operational cost are crucial factors.

An unmanned aerial vehicle (UAV) is an aircraft that can be remotely controlled or autonomously programmed for flight paths without a human pilot on board. Unmanned Aerial Systems (UAS), commonly referred to as UAVs, are equipped with cameras, sensors, communication devices, and other payloads. As the market for UAVs grows and its uses become more varied, there is an increasing need to improve flight capabilities and adaptability for challenging tasks. [1] UAVs were first created for military use, but they are now extensively employed in both military and civilian settings, helping to protect borders and for other purposes. When combined with cutting-edge sensing technologies, their exceptional ability to reach remote or dangerous locations allows for high-resolution imagery for a range of humanitarian and civilian missions [2].

UAVs are divided into two primary categories: rotary-wing UAVs and fixed-wing UAVs, which are categorized according to their design, capabilities, and intended uses. The fixed wing UAVs are renowned for their high cruising speeds while in flight, long endurance, and payload capacity [3], [4]. By affecting variables like lift-to-drag ratio, flight range, and endurance, aerodynamics is essential to maximizing the effectiveness and performance of UAVs. By guaranteeing stability, controllability, and maneuverability, effective aerodynamic considerations allow UAVs to fly for longer periods of time and cover greater ground [5, 6]. Because they produce lift, regulate the lift-to-drag ratio, and affect stall behavior, airfoils are essential to aerodynamics. The air pressure differential between an airfoil's upper and lower surfaces produces the lift force.

Aerodynamic efficiency, in particular a high lift-to-drag ratio ( $Cl/Cd$ ), is crucial for MALE UAVs' long endurance and effective flight performance [7]. Performance, fuel efficiency, and mission duration can all be greatly increased by optimizing airfoil shapes (Austin, 2010).

Though accurate [8], conventional CFD-based design techniques are time-consuming and computationally costly. By learning from CFD data and accurately predicting aerodynamic coefficients, machine learning provides a quick and clever solution to this problem [9].

This project aims to integrate CFD and ML to create a fast, reliable optimization tool for MALE UAV airfoils reducing simulation time while maintaining accuracy.

### **1.3 Objectives of the Project**

The aim of this project is to develop a machine learning-assisted aerodynamic optimization framework for MALE UAV airfoils. The specific objectives include:

1. To run 2D and 3D CFD simulations on a subset of NACA airfoils at various subsonic flow rates and angles of attack.
2. To confirm the accuracy and dependability of simulation results using different tools like XFLR5 or JAVAFOIL.
3. To produce an extensive dataset of the aerodynamic coefficients ( $C_l$  and  $C_d$ ) for training machine learning models and optimization.
4. To put into practice a gradient optimization algorithm based on Python to find airfoil configurations that optimize aerodynamic efficiency.
5. To develop a machine learning model that, given airfoil shapes and flight conditions, can reliably predict  $C_l$  and  $C_d$  values.
6. To develop a predictive tool that eliminates the need to repeat CFD simulations by enabling users to enter the geometry of MALE UAV airfoils and receive estimates of aerodynamic performance.

### **1.4 Scope**

This project uses a hybrid CFD and machine learning approach to optimize the aerodynamic performance of airfoils used in MALE UAVs. Among the main topics discussed are:

- 2D and 3D CFD simulations of specific NACA airfoils at different angles of attack ( $2^\circ$ – $10^\circ$ ) and low subsonic Mach numbers (0.02–0.3).

- CFD results are validated using JAVAFOIL or XFLR5.
- The creation of a gradient optimization algorithm based on Python.
- Developing a machine learning model to forecast aerodynamic coefficients ( $C_l$  and  $C_d$ ).
- Development of a tool that uses user input to estimate airfoil performance.
- Adapting the framework to the unique flight conditions and design requirements of UAVs

## 1.5 Limitations

Notwithstanding the project's breadth and depth, several restrictions were found:

**Types of limited airfoils:** Ten NACA airfoils serve as the basis for the analysis.

**Streamlined flow conditions:** Compressibility, gust response, and transition turbulence were not modeled; only steady-state, incompressible flow was examined.

**Data-driven prediction constraints:** The size and caliber of the training dataset determines how accurate the machine learning model can be.

**Tool range:** The predictive tool may not generalize well to other aircraft classes or high-speed regimes because it is tailored for MALE UAV-related airfoils.

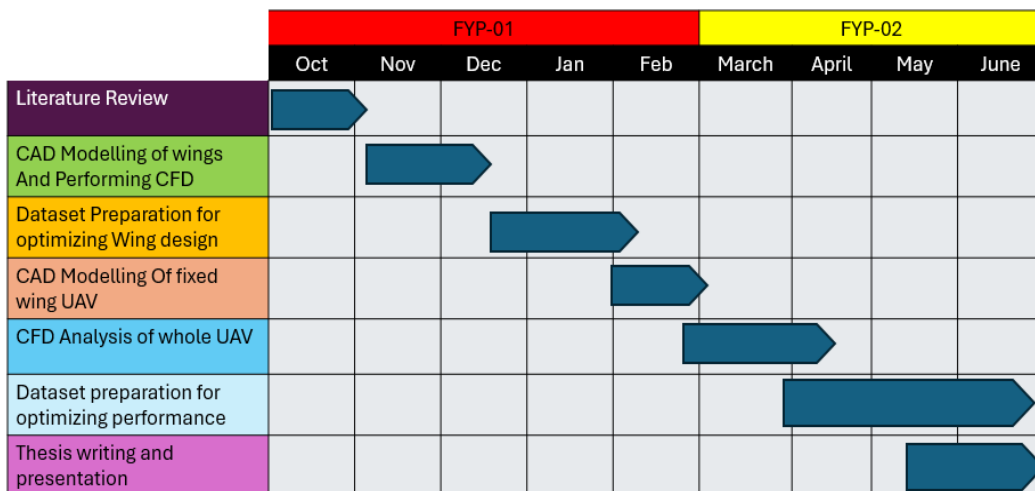


Figure 1.1 Gantt Chart

## **2. Literature Review**

### **2.1 Studies on CFD-Based UAV Optimization**

Because it can accurately predict flow around complex geometries, computational fluid dynamics, or CFD, has become a standard tool in UAV design. Optimizing UAV aerodynamic performance with CFD tools such as ANSYS Fluent and XFLR5 has been the subject of numerous studies. For example, Altug and Kaymaz (2018)[9] optimized a fixed-wing UAV using CFD to improve its lift-to-drag ratio. Similarly, Zhang et al. (2020) [10] examined NACA airfoils for surveillance drones using CFD with an emphasis on enhancing stability and endurance.

These techniques, however, frequently require laborious mesh creation, solver tuning, and post-processing procedures. Hours may pass between each design iteration, particularly when simulating turbulent or unsteady flows.

These techniques, however, frequently require laborious mesh creation, solver tuning, and post-processing procedures. Hours may pass between each design iteration, particularly when simulating turbulent or unsteady flows.

### **2.2 Applications for Machine Learning in Aerodynamics**

Particularly when trained on CFD or experimental data, machine learning (ML) has recently become a potent tool to support aerodynamic predictions. Lift and drag coefficients have been successfully estimated using models such as Gaussian Process Regression (GPR), Artificial Neural Networks (ANNs), and Support Vector Regression (SVR).

For instance, Bhargava et al. (2021) [11] used CFD-generated datasets to create a deep learning model that predicts aerodynamic coefficients. Their findings

demonstrated that ML models can accurately and significantly reduce the computational cost of CFD results. In a different study, Liu et al. (2022) [12] predicted the pressure distribution over airfoils using convolutional neural networks (CNNs), which allowed for quick predictions without meshing.

### **2.3 Summary of Gaps in Current Research**

- Although ML allows for quicker predictions and CFD yields high-fidelity results, a combined framework that utilizes both is still comparatively underdeveloped, particularly for applications unique to MALE UAVs. Most of the current research either investigates ML models using sparse aerodynamic datasets or only focuses on CFD-based optimization.

A glaring gap exists in:

- Using machine learning to integrate validated CFD simulations for real-time aerodynamic prediction.
- Creating lightweight instruments that can be utilized in the early stages of UAV design, customizing optimization for MALE UAV airfoils at low subsonic speeds



### 3. Airfoil Selection

#### 3.1 Airfoil Selection and Geometry Creation

To evaluate and optimize performance for MALE UAVs, **10 NACA airfoils** were selected based on literature and prior aerodynamic studies. These airfoils are commonly used in long-endurance and low-speed UAVs due to their high lift-to-drag characteristics and structural simplicity.

Table 2. 1 Naca Airfoils that are selected based on literature review

<b>NACA 2412</b>	Trainer UAVs, General Aviation UAVs
<b>NACA 4412</b>	Slow-flying UAVs, STOL UAVs
<b>NACA 0012</b>	High-speed UAVs, Tail Sections
<b>NACA 2415</b>	Endurance UAVs, Reconnaissance UAVs
<b>NACA 4415</b>	Agricultural UAVs, Long-Endurance UAVs
<b>NACA 23012</b>	Transport UAVs, MALE UAVs
<b>NACA 2408</b>	Strategic Long-Range UAVs
<b>NACA 43012</b>	Strategic Long-Range UAVs

<b>NACA 23112</b>	Medium Altitude UAVs
<b>NACA 4418</b>	Cargo UAVs, Slow-Speed UAVs

Although the present study focuses on these ten airfoils, **additional airfoils could also be considered** for future analysis. Due to time constraints, only the above-listed airfoils were evaluated in the current phase of the work.

### **3.2 Focus on Cruise Efficiency in Airfoil Evaluation**

Since the objective of this study is to evaluate airfoil performance under operational cruise conditions, the analysis and subsequent optimization are focused on L/D Cruise values rather than L/D Max. This approach ensures that the selected airfoil will deliver optimal endurance and performance during actual missions rather than only under laboratory or ideal conditions.

Figure X presents a comparison of the maximum lift-to-drag ratio (**L/D Max**) and the cruise lift-to-drag ratio (**L/D Cruise**) for the ten selected NACA airfoils.

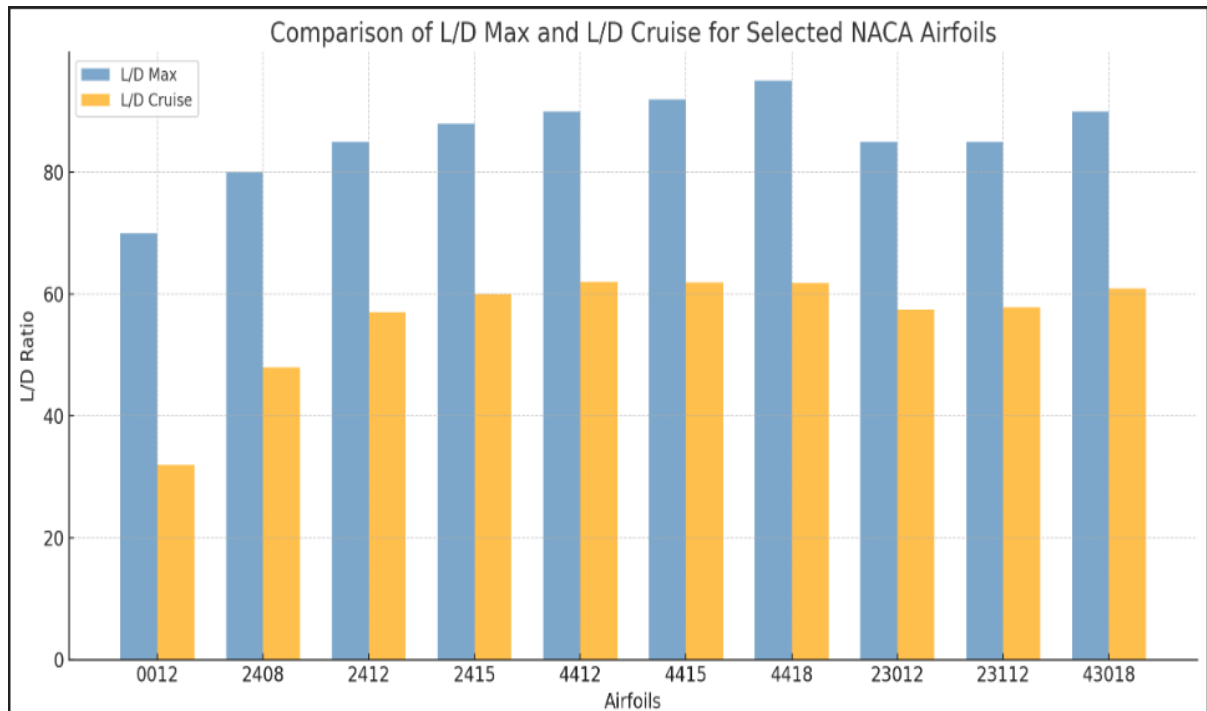


Figure 3. 1 Comparison of L/D Max and L/D Cruise for selected NACA Airfoils

Here is the **bar graph** comparing:

● **L/D Max** (blue bars): the maximum aerodynamic efficiency each airfoil can achieve

● **L/D Cruise** (orange bars): the realistic efficiency during typical UAV cruise

The results indicate that while all airfoils show a reduction in efficiency from L/D Max to L/D Cruise, profiles such as NACA 4415 and NACA 4412 maintain relatively high cruise efficiencies, making them strong candidates for long-endurance UAV applications.

Conversely, airfoils like NACA 0012 exhibit a greater drop in cruise efficiency, suggesting suitability for higher-speed or specialized applications rather than endurance-focused missions.

## **4. Parameters for 2D and 3D Dataset Collection**

Before proceeding to the integration of 3D analysis, it is important to outline the difference in parameters considered during 2D and 3D dataset generation for the developed tool.

### **4.1 2D Analysis Parameters:**

In 2D analysis, the geometry under consideration is a single airfoil section. The input parameters are:

- Chord length (fixed at 1 m)
- Velocity
- Mach number
- Reynolds number

The corresponding output parameters are:

- Coefficient of Lift (CL)
- Coefficient of Drag (CD)

### **4.2 3D Analysis Parameters**

In 3D analysis, the airfoil evolves into a complete wing, introducing additional geometric and aerodynamic parameters. The input parameters expand to:

- Wingspan
- Taper ratio
- Velocity

- Mach number
- Reynolds number

The output parameters remain the same as in the 2D case.

This distinction in parameter set highlights the increased complexity of 3D aerodynamic prediction, as geometric influences such as span and taper ratio begin to play a significant role in the overall aerodynamic performance of the wing.

#### 4.3 CFD-Based Airfoil Analysis

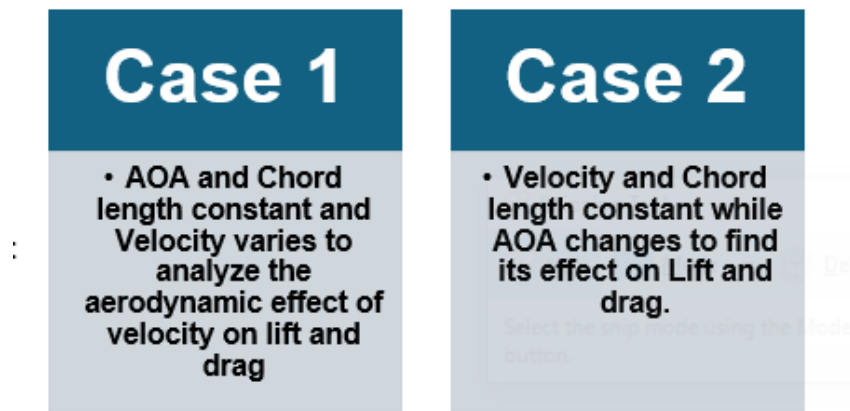


Figure 4.1 Cases for 2D Analysis of Airfoil

In Figure 4.1 2D cases were considered:

1. When the chord length was kept constant and velocity increased, the Mach number increased (AOA remained constant).
2. In another case, the AOA was increased while keeping the velocity constant.

In both cases, the output obtained were CL (lift coefficient) and CD (drag coefficient).

#### 4.4 CFD-Based Wing Analysis

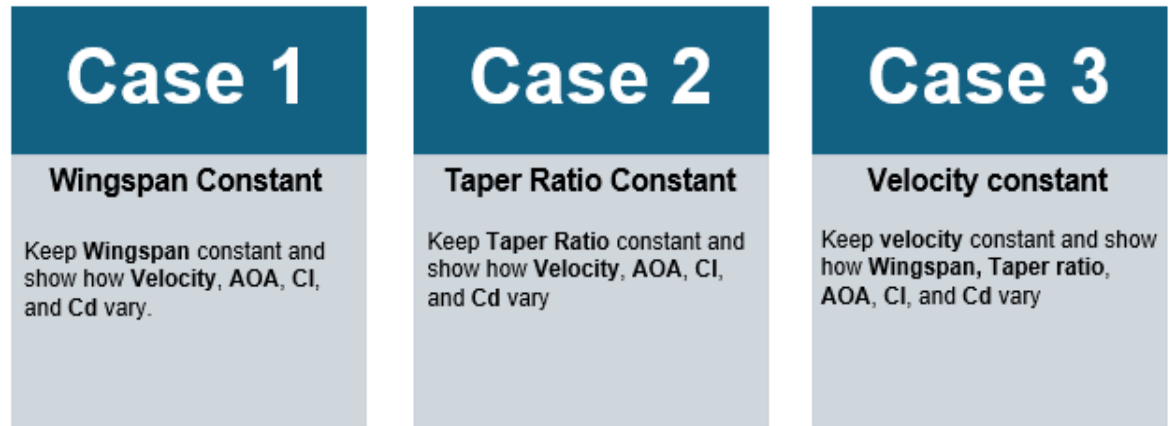


Figure 4. 2 Cases for 3D Analysis of Wings

In Figure 4.2 Three 3D parameter cases were considered:

1. When the taper ratio and wingspan were kept constant and velocity increased, the Mach number increased (AOA remained constant).
2. In another case, the AOA was increased while keeping the velocity constant.

In both cases, the output obtained were CL (lift coefficient) and CD (drag coefficient).

#### 4.5 Constraints of our project

Table 4. 1 Limitations of our simulation tool

<b>Angle of Attack</b>	<b>-2 - 10 (degrees)</b>
<b>Velocity</b>	<b>17m/s-103m/s</b>
<b>Mach Number</b>	<b>0.05-0.3</b>
<b>Chord length</b>	<b>1m</b>

<b>Taper Ratio</b>	<b>1-0.4</b>
<b>Wingspan</b>	<b>2-12m</b>
<b>Reynolds number(3D)</b>	<b><math>10^6 - 10^7</math></b>
<b>Reynolds number(2D)</b>	<b><math>11 \cdot 10^6 - 70 \cdot 10^6</math></b>

#### 4.6 Reason for Limitations

The constraints on Angle of Attack ( $-2^\circ$  to  $10^\circ$ ), Velocity (17 m/s to 103 m/s), and Reynolds Number ( $\leq 10^7$ ) were set to ensure that all analyses remain within the subsonic flow regime, which is representative of MALE UAV cruise conditions.

Another reason for these constraints is that the current phase of the project focuses only on cruise conditions. However, the project is open-ended and can be extended in the future to include other flight regimes beyond cruise, such as climb, descent, and maneuvering conditions.

## 5. Simulation Tools and their working

For the aerodynamic analysis, two tools were employed: **ANSYS Fluent** and **XFLR5**.

Half of the selected airfoils were simulated in ANSYS, while the remaining half were analyzed using XFLR5. To validate the consistency of results, one airfoil was analyzed using both tools, and the outcomes were found to be in close agreement. This verification confirmed the reliability of both approaches, providing the basis for using the two tools in parallel for the simulations.

### 5.1 XFLR5 Approach

In the case of XFLR5, **two different analysis approaches** were applied depending on the dimensionality of the model:

#### 5.1.1 2D Analysis:

Conducted using the Foil Analysis module in XFLR5, focusing on individual airfoil sections to determine their aerodynamic coefficients.

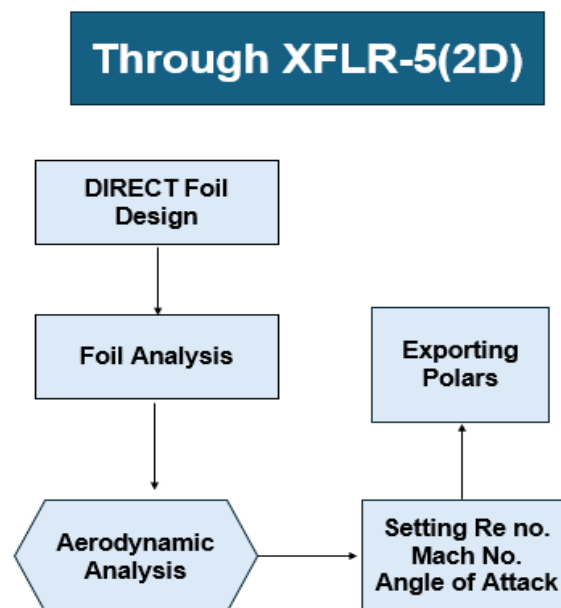


Figure 5. 1 2D Airfoil Analysis in XFLR5



### 5.1.2 3D Analysis:

Figure 5.2 shows Simulation conducted using the *Vortex Lattice Method (VLM)*, also known as the **Horseshoe Vortex Method**, to simulate complete wing geometries and capture three-dimensional aerodynamic effects.

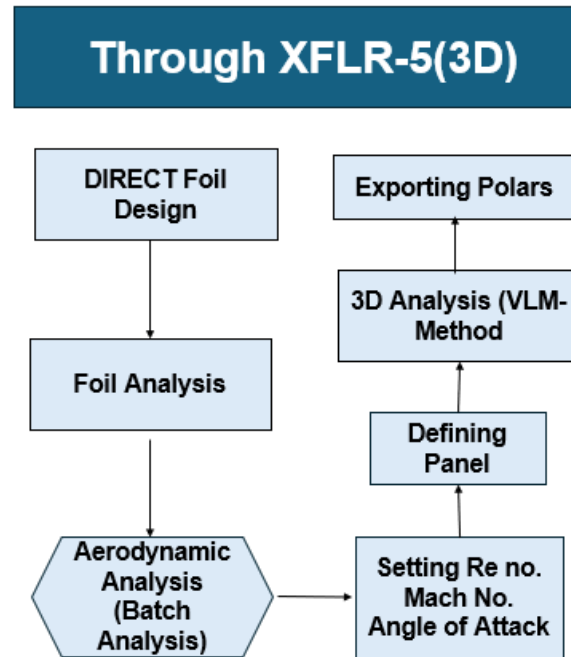


Figure 5. 2 3D Wing Analysis in XFLR5

Each profile was modeled to maintain geometric accuracy, consistent chord length, wingspan and taper ratio for comparison.

## 5.2 Ansys Approach

The **CFD simulation flowchart** outlines the key steps followed in the simulation process:

1. **Problem Definition:** Define the study (airfoils) and simulation conditions (Mach number, angles of attack).

2. **Geometry Creation:** Create the 2D airfoil geometry (e.g., NACA airfoils) in **SolidWorks**.
3. **Meshing:** Generate the mesh in **ANSYS Fluent**, applying structured grids and refining the boundary layer.
4. **Boundary & Initial Conditions:** Set boundary conditions (inlet, outlet, walls) and initial conditions (velocity, pressure).
5. **Solver Setup:** Select the appropriate solver and turbulence model, then configure settings for steady-state simulations.
6. **Simulation:** Run the simulations across different Mach numbers and angles of attack.
7. **Results Analysis:** Analyze the lift and drag characteristics, then validate the results.

Figure 5.3 shows the 2D Airfoil domain in ansys and this domain is followed for all airfoils.

CFD simulations were conducted to analyze the **lift** and **drag characteristics** of the selected airfoils under low subsonic conditions, which are typical of **MALE UAV** flight regimes.

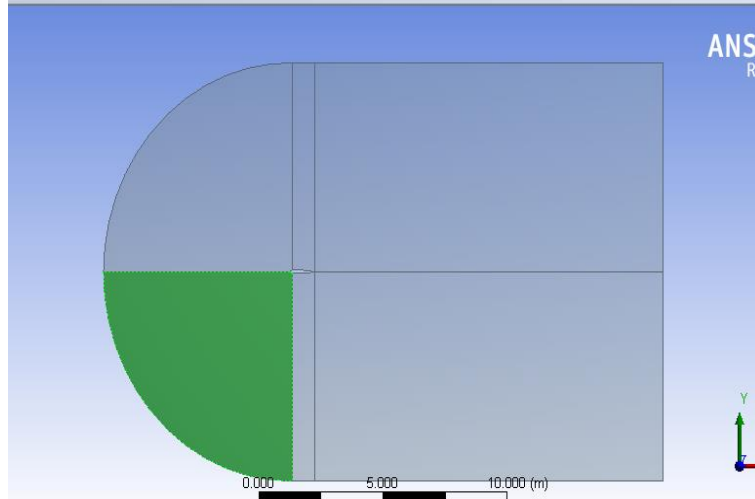


Figure 5. 3 2D Domain

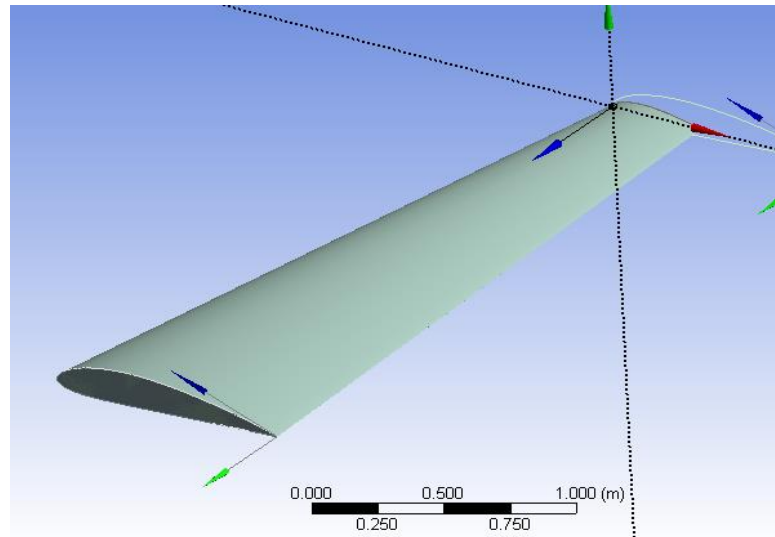


Figure 5. 4 3D Geometry in Ansys

**Meshing Software:** The mesh generation was performed using **ANSYS Fluent** due to its robust capabilities in structured and unstructured meshing, as well as its flexibility in boundary layer refinement.

### 5.2.1 Mesh Type:

- **O-grid** and **C-grid** structured meshes were used to improve the accuracy of the simulations.
- **Boundary layer meshing** was implemented to accurately capture the near-wall effects, ensuring that the flow behavior close to the surface was well-represented.

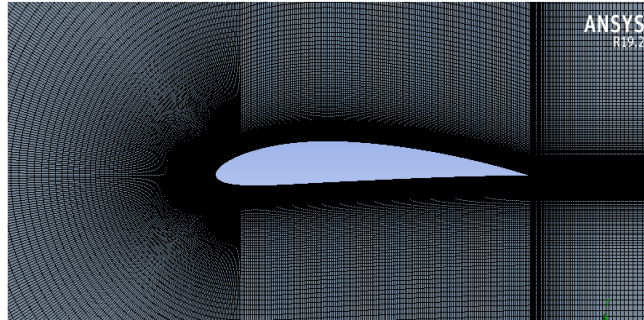


Figure 5. 5 Mesh at the boundary of the airfoil

- $Y^+ < 1$  was maintained in regions where boundary layer refinement was critical to capture the viscous effects effectively.

Mesh Quality	
Maximum Skewness	0.78
Max Aspect ratio	3200

Mesh Statistics	
No. of nodes	21940

Figure 5. 6 Mesh Quality

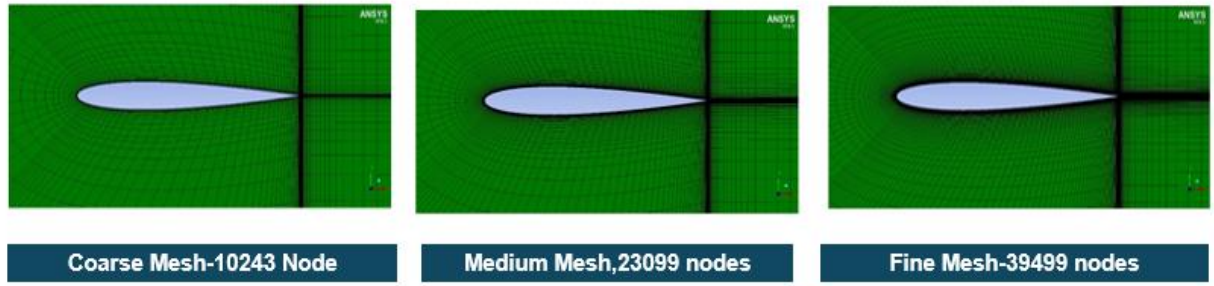


Figure 5. 7 mesh refinement

Coarse, medium, and fine meshes were tested to evaluate their effect on **CL** and **CD** values. The coarse mesh gave less accurate results, the medium mesh improved accuracy, and the fine mesh provided stable and reliable values. Therefore, the **fine mesh** was used for all final simulations.

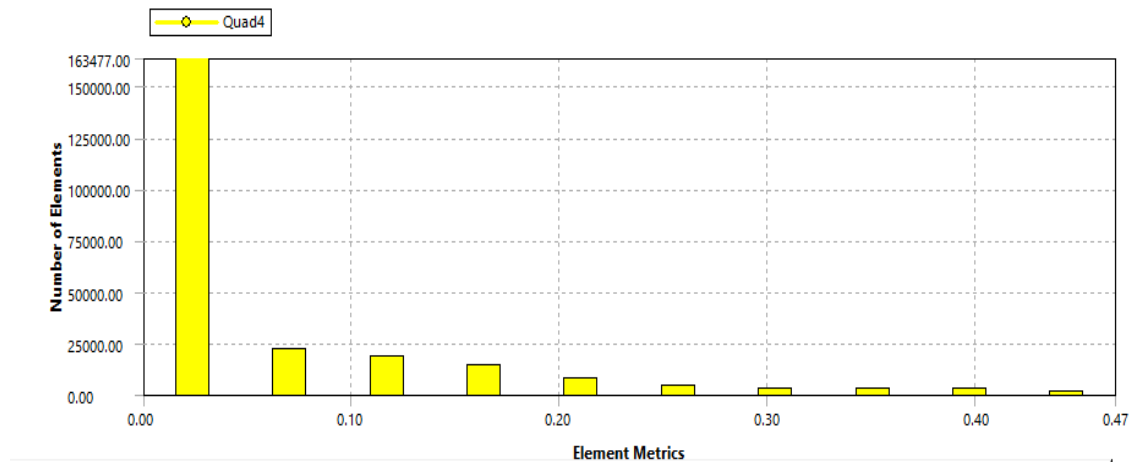


Figure 5. 8 Mesh Skewness Study

### 5.3 Parametric Method:

A **parametric method** was applied to systematically explore the effect of different **angles of attack (AoA)** and **Mach numbers** on the aerodynamic characteristics of

the airfoils. This method involved varying the following parameters across multiple simulations:

- **Mach Number Range:** 0.02 to 0.3
- **Angle of Attack (AoA):** 2° to 10°

Each combination of these parameters was run to understand how changes in flight conditions influence the **lift** and **drag** performance.

Table of Design Points					
	A	C	D	E	F
1	Name ▾	P2 - parameter-2 ▾	P3 - y velocity ▾	P4 - cd-op ▾	P5 - cl-op ▾
2	Units	m s <sup>-1</sup> ▾	m s <sup>-1</sup> ▾		
11	DP 8	38.655	2.703	-0.0040228	1.5117
12	DP 9	38.538	4.05	-0.062078	2.0591
13	DP 10	38.328	5.392	-0.1403	2.5955
14	DP 11	38.161	6.7288	-0.23849	3.13
15	DP 12	41.745	0	0.058668	0.46723
16	DP 13	41.725	1.457	0.038352	1.1122
17	DP 14	41.648	2.9123	-0.0055856	1.7545
18	DP 15	41.521	4.364	-0.073064	2.391
19	DP 16	41.343	5.8104	-0.16397	3.0193
20	DP 17	41.116	7.2498	-0.27815	3.6367
21	DP 18	45.75	0	0.069194	0.5575
22	DP 19	45.722	1.59	0.04497	1.3303
23	DP 20	45.639	3.191	-0.007971	2.1062
24	DP 21	45.499	4.782	-0.089108	2.8721

Figure 5. 9 Parametric approach in Ansys

The parametric approach allowed for efficient exploration of multiple configurations, leading to a deeper understanding of the aerodynamic behavior across different operating conditions.

## **6.Validation of Results and Data Extraction**

Validation was carried out for airfoils, namely NACA 4412 and NACA 0012, using experimental data and theoretical techniques to guarantee the accuracy of the simulation results obtained from ANSYS Fluent and XFLR5.

### **6.1 Validation Method:**

For the NACA 4412 and NACA 0012 airfoils, the lift and drag coefficients ( $C_l$  and  $C_d$ ) derived from the simulations were contrasted with experimental and theoretical findings. Because of their widespread application in aerodynamic research, these airfoils were chosen to provide accurate experimental data for comparison.

#### **6.1.1 Experimental Data Comparison:**

- The simulated  $C_l$  vs. AoA and  $C_d$  vs. AoA curves for the NACA 4412 and NACA 0012 airfoils were compared to experimental results from wind tunnel tests and literature. The  $C_l$  and  $C_d$  values from the simulations were directly compared to experimental measurements for different angles of attack (AoA).

#### **6.1.2 NACA 4412 Validation:**

Figure 6.1 and 6.2 shows NACA 4412 airfoil was validated for angles of attack ranging from  $0^\circ$  to  $10^\circ$ . The simulation results for  $C_L$  and  $C_D$  were compared with reference data to ensure accuracy. The trends observed in lift and drag coefficients closely matched the theoretical and experimental data, confirming the reliability of the aerodynamic analysis setup

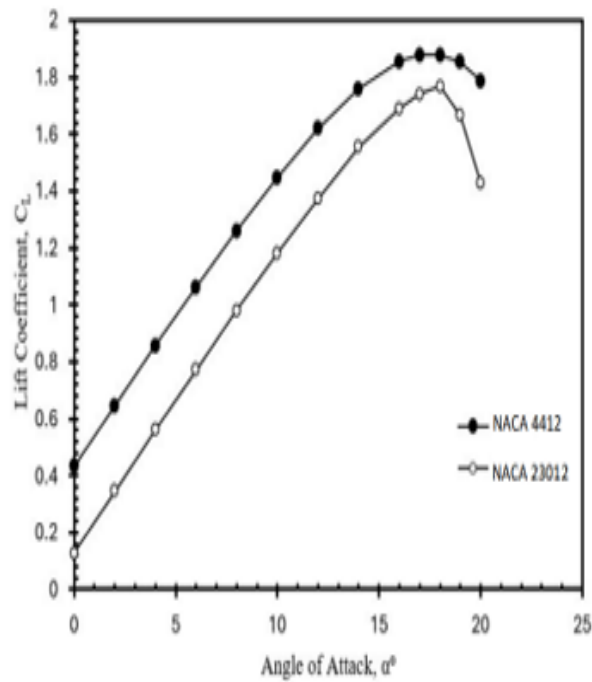


Figure 6. 2 Paper graph of naca 4412

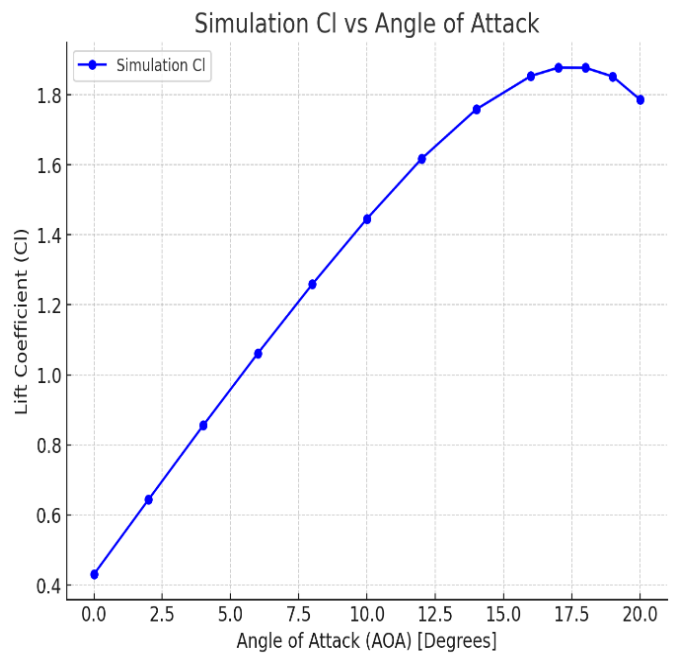


Figure 6. 1 MATLAB Graph validated- Naca 4412

### 6.1.3 NACA 0012 Validation

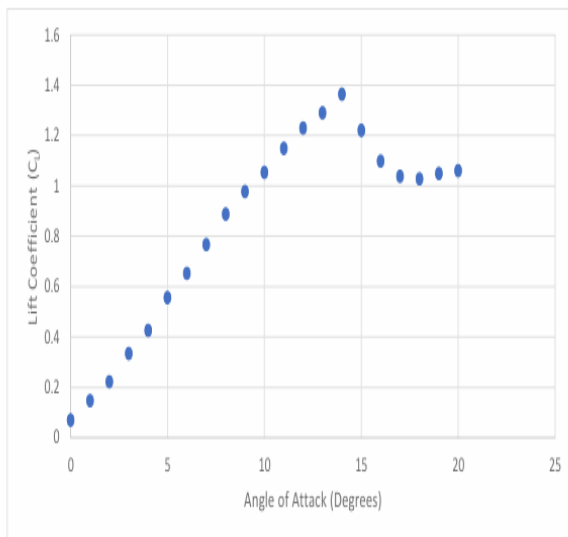


Figure 6. 3 Paper Graph of naca 0012

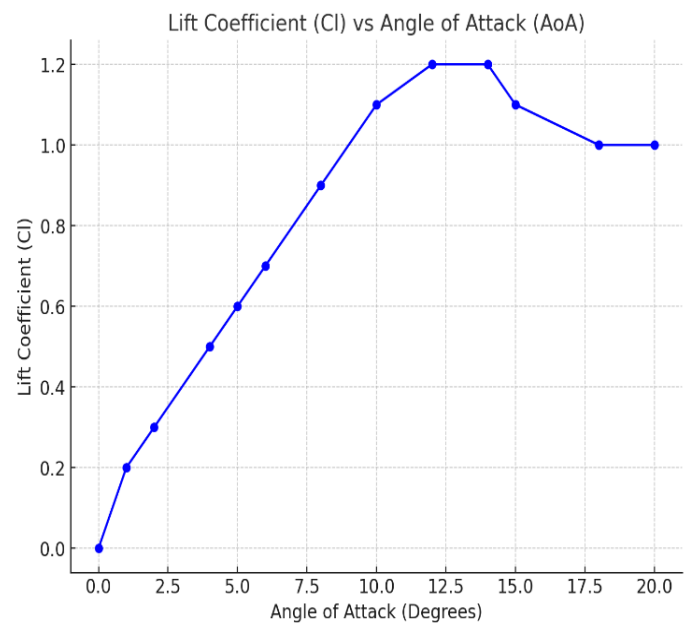


Figure 6. 4 MATLAB Graph of Naca 0012-Validated



Figure 6.3 and 6.4 shows NACA 0012 airfoil validations for angles of attack ranging from  $0^\circ$  to  $10^\circ$ . The simulation results for CL and CD were compared with reference data from a NASA research paper to verify accuracy. The lift and drag trends showed close agreement with the published data, confirming the validity of the aerodynamic analysis method used

## 6.2 Data Collection:

- Collected a large dataset of **Cl and Cd values** in an **Excel sheet**, which includes simulation results for different airfoils, **AoA**, and **Mach numbers**

### 6.2.1 2D Dataset

Mach	Re	alpha	CL	CD	Airfoil	velocity	max_thickness
0.05	1135000	-2	0.2443	0.0083	0	17	0.18
0.05	1135000	-1	0.3540	0.0082	0	17	0.18
0.05	1135000	0	0.4638	0.0082	0	17	0.18
0.05	1135000	1	0.5702	0.0079	0	17	0.18
0.05	1135000	2	0.6763	0.0078	0	17	0.18
0.05	1135000	3	0.7781	0.0077	0	17	0.18
0.05	1135000	4	0.8940	0.0081	0	17	0.18
0.05	1135000	5	1.0320	0.0087	0	17	0.18
0.05	1135000	6	1.1144	0.0091	0	17	0.18
0.05	1135000	7	1.1989	0.0098	0	17	0.18
0.05	1135000	8	1.2860	0.0107	0	17	0.18
0.07	1630000	-2	0.2473	0.00771	0	24	0.18
0.07	1630000	-1	0.3593	0.00765	0	24	0.18
0.07	1630000	0	0.4708	0.0076	0	24	0.18
0.07	1630000	1	0.5814	0.0075	0	24	0.18
0.07	1630000	2	0.6886	0.0073	0	24	0.18
0.07	1630000	3	0.7977	0.00714	0	24	0.18
0.07	1630000	4	0.8979	0.00723	0	24	0.18
0.07	1630000	5	1.0279	0.00781	0	24	0.18

Figure 6. 5 2D Dataset (1)

172	0.27	6290000	-1	0.1040	0.00473	9	92	0.18
173	0.27	6290000	0	0.0000	0.0048	9	92	0.18
174	0.27	6290000	1	0.1040	0.00473	9	92	0.18
175	0.27	6290000	2	0.2111	0.00501	9	92	0.18
176	0.27	6290000	3	0.3151	0.00532	9	92	0.18
177	0.27	6290000	4	0.4199	0.00554	9	92	0.18
178	0.27	6290000	6	0.6758	0.00673	9	92	0.18
179	0.27	6290000	7	0.8052	0.00784	9	92	0.18
180	0.3	6900000	-2	-0.2139	0.0051	9	103	0.18
181	0.3	6900000	-1	-0.1059	0.0048	9	103	0.18
182	0.3	6900000	0	0.0000	0.0048	9	103	0.18
183	0.3	6900000	1	0.1059	0.0048	9	103	0.18
184	0.3	6900000	2	0.2139	0.0051	9	103	0.18
185	0.3	6900000	3	0.3207	0.0054	9	103	0.18
186	0.3	6900000	4	0.4259	0.0055	9	103	0.18
187	0.3	6900000	5	0.5409	0.0058	9	103	0.18
188	0.3	6900000	6	0.6621	0.0068	9	103	0.18
189	0.3	6900000	7	0.8128	0.0078	9	103	0.18
190	0.3	6900000	8	0.8920	0.0084	9	103	0.18
191								

Figure 6. 6 2D Dataset (2)

## 6.2.2 3D Dataset

1	Wingspan	MAC	Taper Ratio	Velocity	AOA	Cl	Cd	Airfoil	Reynolds Num	Mach Num
2	2	1.25	1	17	-2	0.051856	0.005281	0	1,454,000	0.30
3	2	1.25	1	17	-1	0.090413	0.006052	0	1,454,000	0.05
4	2	1.25	1	17	0	0.128897	0.007431	0	1,454,000	0.05
5	2	1.25	1	17	1	0.167267	0.009345	0	1,454,000	0.05
6	2	1.25	1	17	2	0.205481	0.01191	0	1,454,000	0.05
7	2	1.25	1	17	3	0.2435	0.0152	0	1,454,000	0.05
8	2	1.25	1	17	4	0.281284	0.019294	0	1,454,000	0.05
9	2	1.25	1	17	5	0.318792	0.02413	0	1,454,000	0.05
10	2	1.25	1	17	6	0.355987	0.029511	0	1,454,000	0.05
11	2	1.25	1	17	7	0.39283	0.035381	0	1,454,000	0.05
12	2	1.25	1	17	8	0.064402	0.00665	0	1,454,000	0.05
13	4	1.25	1	17	-2	0.12263	0.007496	0	1,454,000	0.05
14	4	1.25	1	17	-1	0.180773	0.008988	0	1,454,000	0.05
15	4	1.25	1	17	0	0.238778	0.011163	0	1,454,000	0.05
16	4	1.25	1	17	1	0.296595	0.014037	0	1,454,000	0.05
17	4	1.25	1	17	2	0.354172	0.017651	0	1,454,000	0.05
18	4	1.25	1	17	3	0.411459	0.021949	0	1,454,000	0.05
19	4	1.25	1	17	4	0.468406	0.026923	0	1,454,000	0.05
20	4	1.25	1	17	5	0.524964	0.032556	0	1,454,000	0.05
21	4	1.25	1	17	6	0.581084	0.038821	0	1,454,000	0.05
22	4	1.25	1	17	7	0.071647	0.006541	0	1,454,000	0.05
23	4	1.25	1	17	8	0.140958	0.007259	0	1,454,000	0.05
24	6	1.25	1	17	-2	0.210182	0.008596	0	1,454,000	0.05
25	6	1.25	1	17	-1	0.279265	0.010641	0	1,454,000	0.05
26	6	1.25	1	17	0	0.348154	0.013413	0	1,454,000	0.05
27	6	1.25	1	17	1	0.416796	0.016894	0	1,454,000	0.05
28	6	1.25	1	17	2	0.485138	0.021063	0	1,454,000	0.05
29	6	1.25	1	17	3	0.553128	0.025908	0	1,454,000	0.05

Figure 6. 7 3D Dataset (1)

28054	8	1.35	0.4	103	0	0	0.004976	9	9,888,000	0.30
28055	8	1.35	0.4	103	1	0.075452	0.00516	9	9,888,000	0.30
28056	8	1.35	0.4	103	2	0.150849	0.006137	9	9,888,000	0.30
28057	8	1.35	0.4	103	3	0.226135	0.007854	9	9,888,000	0.30
28058	8	1.35	0.4	103	4	0.301257	0.010181	9	9,888,000	0.30
28059	8	1.35	0.4	103	5	0.376158	0.013056	9	9,888,000	0.30
28060	8	1.35	0.4	103	6	0.450784	0.016507	9	9,888,000	0.30
28061	8	1.35	0.4	103	7	0.525083	0.020576	9	9,888,000	0.30
28062	8	1.35	0.4	103	8	0.599001	0.025419	9	9,888,000	0.30
28063	10	1.35	0.4	103	-2	-0.16186	0.006067	9	9,888,000	0.30
28064	10	1.35	0.4	103	-1	-0.08096	0.005127	9	9,888,000	0.30
28065	10	1.35	0.4	103	0	0	0.004976	9	9,888,000	0.30
28066	10	1.35	0.4	103	1	0.080958	0.005127	9	9,888,000	0.30
28067	10	1.35	0.4	103	2	0.161861	0.006067	9	9,888,000	0.30
28068	10	1.35	0.4	103	3	0.242655	0.007678	9	9,888,000	0.30
28069	10	1.35	0.4	103	4	0.323286	0.009844	9	9,888,000	0.30
28070	10	1.35	0.4	103	5	0.403701	0.012503	9	9,888,000	0.30
28071	10	1.35	0.4	103	6	0.483845	0.015704	9	9,888,000	0.30
28072	10	1.35	0.4	103	7	0.563667	0.019579	9	9,888,000	0.30
28073	10	1.35	0.4	103	8	0.643112	0.024149	9	9,888,000	0.30
28074	12	1.35	0.4	103	-2	-0.16988	0.005994	9	9,888,000	0.30
28075	12	1.35	0.4	103	-1	-0.08497	0.005098	9	9,888,000	0.30
28076	12	1.35	0.4	103	0	0	0.004976	9	9,888,000	0.30
28077	12	1.35	0.4	103	1	0.084965	0.005098	9	9,888,000	0.30
28078	12	1.35	0.4	103	2	0.169878	0.005994	9	9,888,000	0.30
28079	12	1.35	0.4	103	3	0.254684	0.007502	9	9,888,000	0.30
28080	12	1.35	0.4	103	4	0.33933	0.009507	9	9,888,000	0.30
28081	12	1.35	0.4	103	5	0.423764	0.011963	9	9,888,000	0.30
28082	12	1.35	0.4	103	6	0.507934	0.014925	9	9,888,000	0.30

Figure 6. 8 3D Dataset (2)

### 6.3 Data Conversion:

Converted the **Excel sheet data** into a format suitable for further analysis and use in **machine learning algorithms** for optimization.

## 7. Predicting Machine Learning Model

For predicting the aerodynamic performance of MALE UAV airfoils, **multiple regression** is the ideal model. Since **Cl** and **Cd** values are continuous, not categorical, regression is well-suited for capturing the gradual variation in airfoil performance. It allows us to model the relationship between input parameters (e.g., AoA, Mach number) and the aerodynamic coefficients. This approach helps develop a **machine learning-based aerodynamic prediction tool**, which can predict **Cl** and **Cd** for different airfoils, enabling optimization for better UAV performance.

### Regression

► From features to predictions;

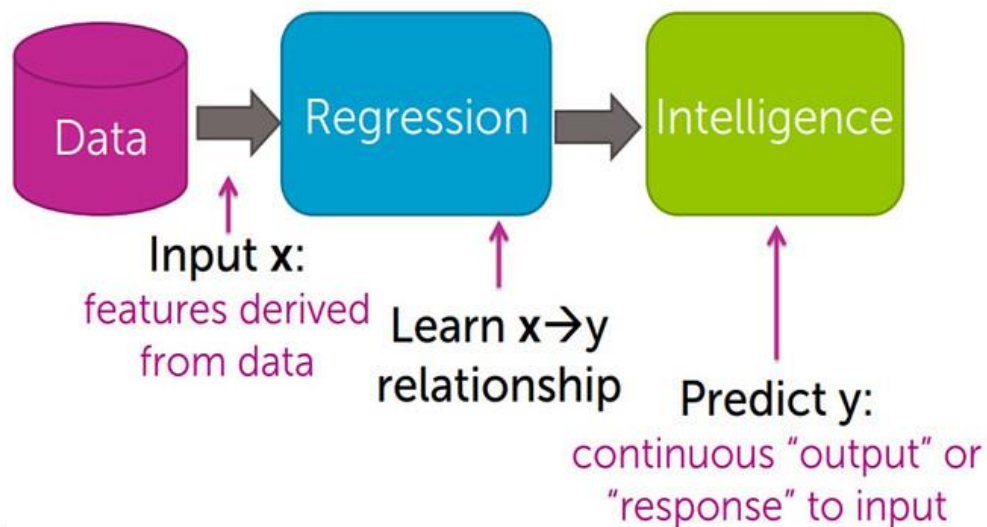




Figure 7. 1 Regression overview

Table 7. 1 Diff b/w Classification and Regression

<i>Aspects</i>	<i>Classification</i>	<i>Regression</i>
Definition	Predicts <b>categorical</b> labels (e.g., "stall" or "no stall").	Predicts <b>continuous</b> numerical values (e.g., Cl, Cd).
Output Type	Discrete classes (e.g., 0 or 1, Yes or No).	Continuous values (e.g., Lift Coefficient, Drag Coefficient)
Use Case	Used for spam detection, image recognition, etc.	Aerodynamics, Weather Forecasting
Best For FYP		

## 7.1 Multiple Regression

- We are predicting aerodynamic performance (**Cl, Cd values**), which are **continuous** rather than categorical.
- Airfoil performance varies **gradually**, requiring a model that captures trends, not just classes.

Regression allows us to develop an **ML-based aerodynamic prediction tool** for MALE UAV airfoils.

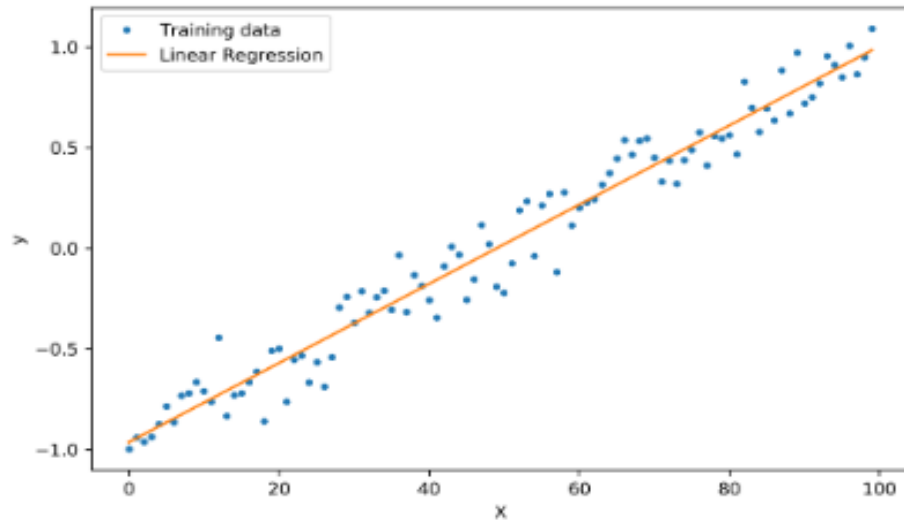


Figure 7. 2 Multiple regression generated graph

The following occurs in a multiple regression linear graph, which is typically a scatter plot with a line:

The actual observed values from your dataset, or what you actually measured, are represented by dots (points) as shown in figure 7.2

Line of regression → This displays the values that your regression model predicted.

Table 7. 2 Types of Optimizers

Features	Particle Swarm Optimizer	Genetic Algorithm	Gradient Based Optimizer
Types	Stochastic (Random Based)	Stochastic (Evolutionary Based	Deterministic

<b>Convergence speed</b>	Slower (requires multiple iterations of swarm movement)	Slower (requires mutation, crossover, selection)	<b>Faster</b> (uses derivatives to move toward optimal solution)
<b>Computational Cost</b>	<b>Higher</b>	Higher	Lower
<b>Accuracy</b>	Moderate	Moderate	High
<b>Best For</b>	Multi-modal, complex landscapes	Problems with unknown/noisy gradients	<b>Smooth, continuous functions</b> with clear gradients

## 7.2 Gradient-Based Optimization

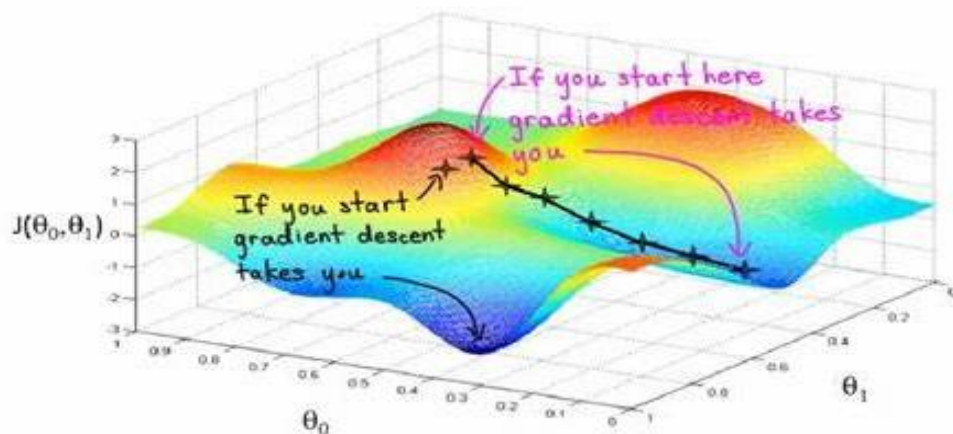


Figure 7. 3 Gradient Based Optimizer

Figure 7.3 shows that gradient based optimizer:

- ❖ **Faster convergence** (few iterations needed)
- ❖ **More precise** (reaches the exact local/global optimum)
- ❖ **Computationally efficient** (fewer function evaluations)
- ❖ **L/D and Range equations are differentiable** (making gradients useful)

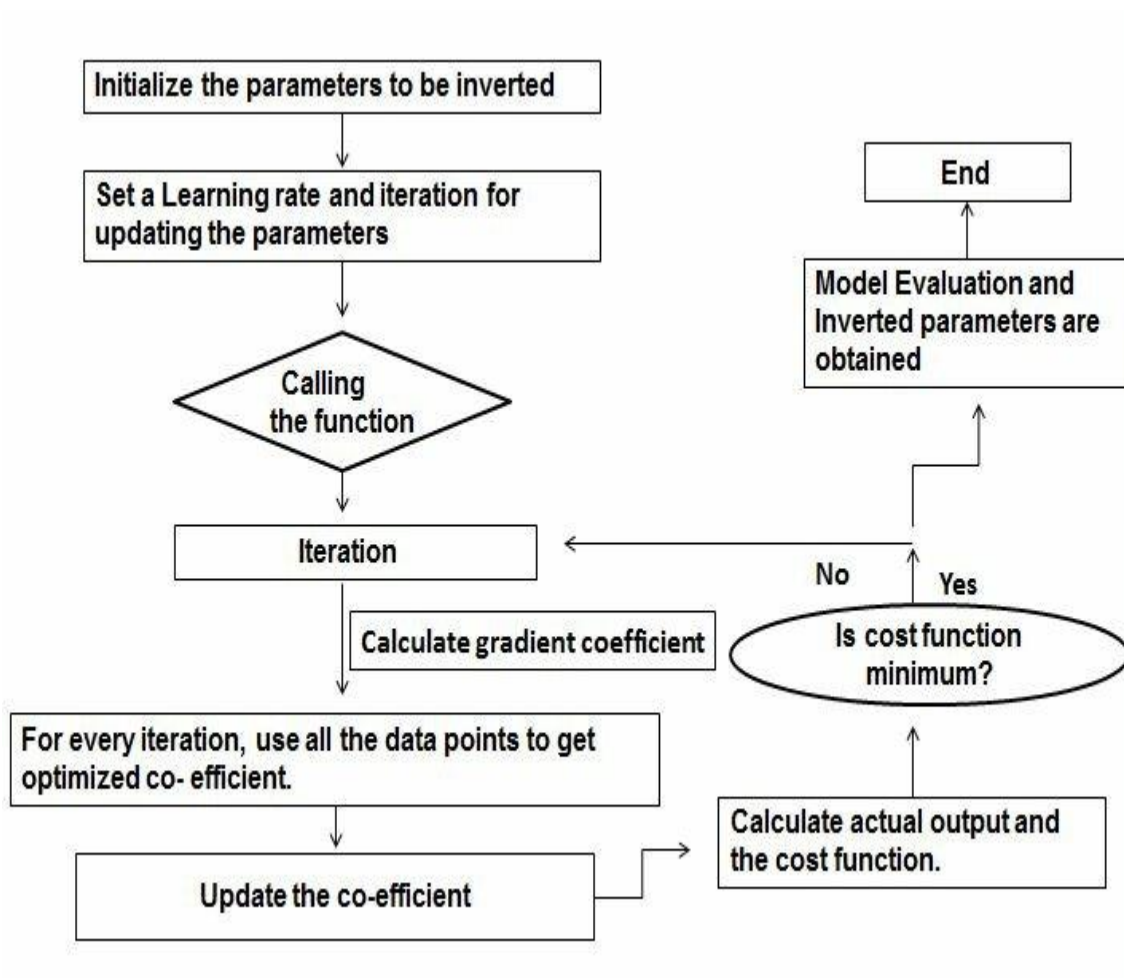


Figure 7. 4 Generic flowchart of gradient based optimizer



## 8. Performance optimizer for UAVs

A pinch to develop a performance optimizer for UAVs was to optimize the performance parameters of UAVs including Range, Endurance and aerodynamic efficiency.

There are a lot of techniques of optimization, but gradient based optimizer was used due to its faster convergence speed because it uses derivatives in code to move towards optimal solution, it has lower computational cost and is best for smooth continuous functions with clear gradients.

Any optimizer includes three parts:

### 8.1 Objective Function:

- Maximizing L/D ratio (aerodynamic efficiency)

$$\frac{L}{D} = \frac{cl}{cd}$$

#### 8.1.1 Optimizing Range of UAVs

Using Range eq from Anderson book of Performance:

$$R = \eta_p / c * \left(\frac{L}{D}\right) g \cdot \ln\left(\frac{W_i}{W_f}\right)$$

#### 8.1.2 Drag Model (Raymer's approach):

$$CD = CD_0 + KC_l^2$$

#### 8.1.3 Optimizing endurance of UAVs

Using Endurance eq from Anderson book of Performance:

$$R = \eta_p / c * \left(\frac{cl^{\frac{3}{2}}}{cd}\right) \cdot \sqrt{\frac{2}{w}}$$

## 8.2 Design Variables:

- Taper ratio
- Aspect Ratio

### 8.2.1 Constraints:

- The limit:  $5 < AR < 20$
- Coefficient of Lift (0.3 – 1.5)

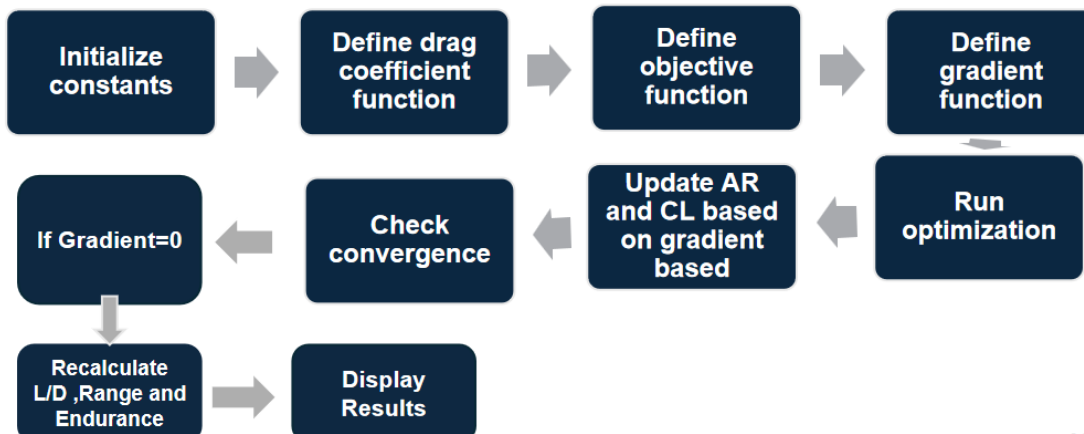


Figure 8. 1 Flowchart of working of Performance optimizer

## 8.3 Output of Code:

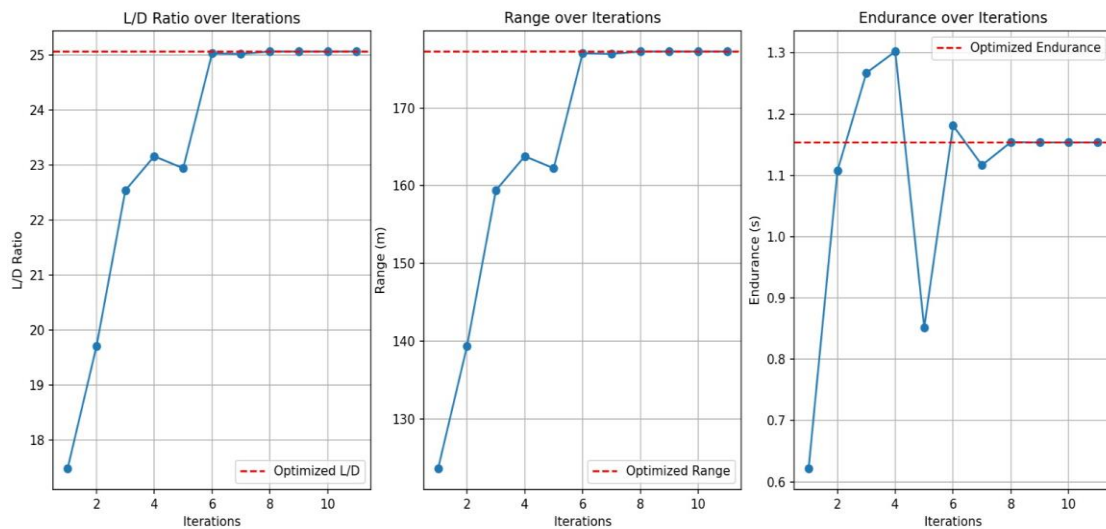


Figure 8. 2 Optimized L/D Range and Endurance

#### **8.4 Conclusion:**

This graph confirms that the gradient-based optimization successfully found the optimal aerodynamic design for maximizing L/D, range and endurance.

The optimization process is efficient, reaching near-optimal values within 10 iterations.

The optimizer avoids overfitting or instability, as the values remain stable in later iterations.

## 9. Machine learning model training

For 2D dataset, it was trained using different Regression models because according to our dataset it acquires continuous values and also inputs and outputs both were given in the dataset .So under supervised based learning ,different regression models were applied to it in order to determine the best accuracy .This dataset was of 1200 datapoints including Mach ,Re ,Angle of attack ,Airfoil ,Velocity and max thickness ( according to selected airfoil ) as input features and CL ,CD as output features .

### 9.1 Regression Algorithms applied:

#### 9.1.1 Random forest:

Random Forest is an ensemble learning method used for both classification and regression tasks. It creates a forest (collection) of decision trees and makes predictions by averaging the predictions of the individual trees (for regression)

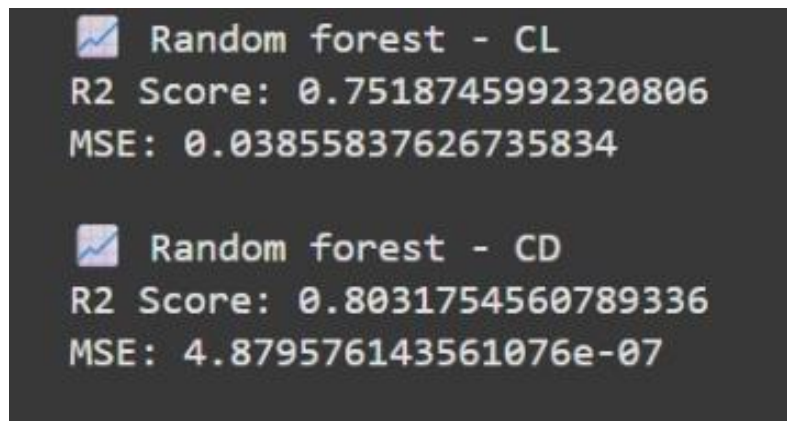


Figure 9. 1 Random Forest for 2D Dataset

#### 9.1.2 Multiple linear regression:

MLR is a statistical technique used to model the relationship between a dependent variable (Y) and multiple independent variables (X1, X2, ... Xn). It assumes a linear relationship between the inputs and output.

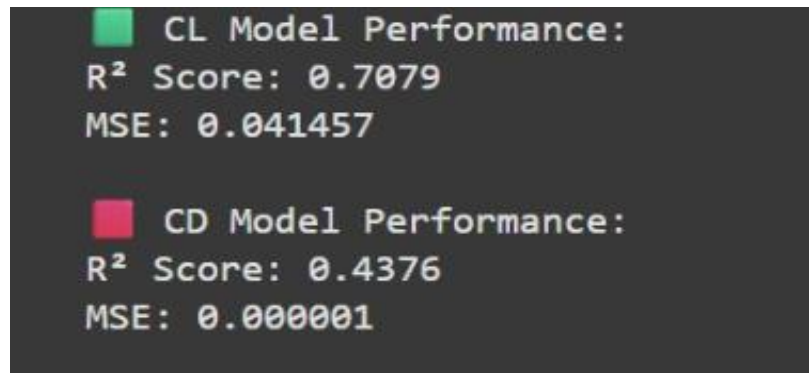


Figure 9. 2 Multiple regression for 2DDataset

### 9.1.3 XG – boost Regressor

XG Boost is an implementation of gradient boosting that is particularly efficient for complex relationships. It builds an ensemble of decision trees, where each tree tries to correct the errors of the previous tree.

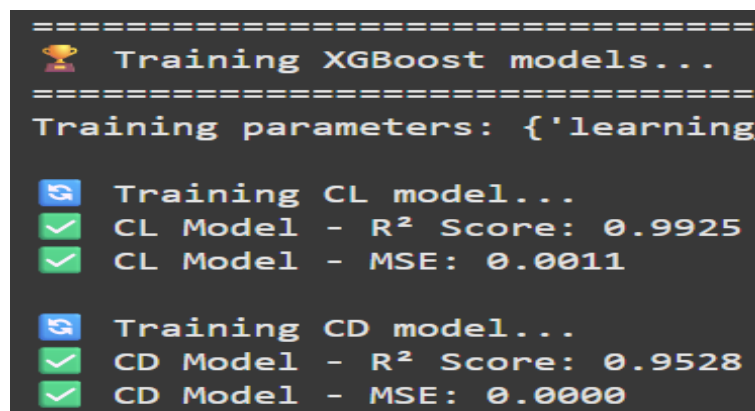


Figure 9. 3 XG-Boost regressor for 2D Dataset

### 9.1.4 Support Vector Regressor:

Use when your data is non-linear and you have high-dimensional or complex data. SVR works well in these situations but can be slow for large datasets.

	Model	R2 Score	MSE
0	SVR - CL	0.696032	4.313482e-02
1	SVR - CD	0.646181	5.850682e-07

Figure 9. 4 Support vector regressor for 2D Dataset

## 9.2 For 3D Dataset:

For 3D dataset, it was of 28000 datapoints including wingspan, Mean Aerodynamic chord, taper ratio, velocity, angle of attack, wings, Re no. ,Mach no. as input features and CL, CD as output features. The regression models which were applied to this dataset were only that which can handle large datasets easily.

### 9.2.1 Random forest:

Random Forest Regression is an ensemble method that builds multiple decision trees and averages their predictions to provide a more accurate and stable result for continuous values.



 <b>Random Forest for Cl</b> R2 Score: 0.9710419358730993 MSE: 0.005062927157835334
 <b>Random Forest for Cd</b> R2 Score: 0.9792475769801204 MSE: 1.9499582437000454e-06

Figure 9. 5 Random Forest for 3D Dataset

### 9.2.2 Gradient boost:

Gradient Boosting Regression is a technique that builds decision trees sequentially, each correcting the errors of the previous one, to predict continuous values.

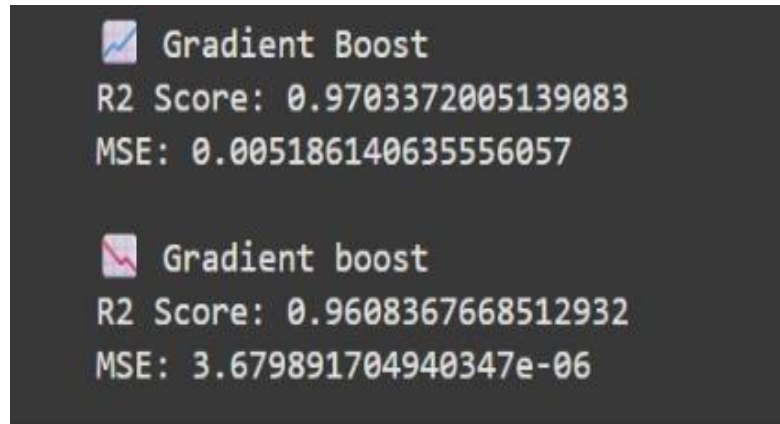


Figure 9. 6 Gradient boost for 3D Dataset

### 9.3 Conclusion:

As observed from above data, our airfoils dataset generated from cfd software was best trained by applying Xg -boost Regressor with 99% accuracy (R2 score) value for CL trained and 95% accuracy (R2 score) value for CD.

On the other hand, our wing dataset was best trained by applying random forest with 97% accuracy (R2 score) value for CL and 98% accuracy (R2 score) value for CD.

## 2D Regression Model Performance

Model	R <sup>2</sup> Score (CL)	R <sup>2</sup> Score (CD)
Multiple Linear Reg.	0.7079	0.4376
Random Forest	0.7524	0.801
SVR Regression	0.6960	0.6462
<b>XG boost regressor</b>	<b>0.9925</b>	<b>0.9528</b>

## 3D Regression Model Performance

Model	R <sup>2</sup> Score (CL)	R <sup>2</sup> Score (CD)
Gradient Boost	0.9703	0.9608
<b>Random Forest</b>	<b>0.9710</b>	<b>0.9792</b>

Figure 9. 7 A comparison of different models with their R<sup>2</sup>



So, for 2D -XG Boost Regressor:

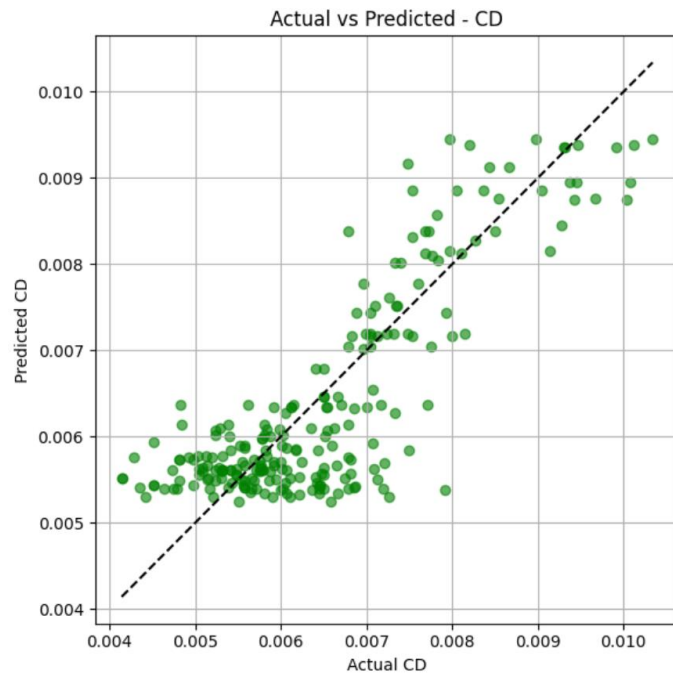


Figure 9. 8 XG Boost Regression Graph for 2D-CD

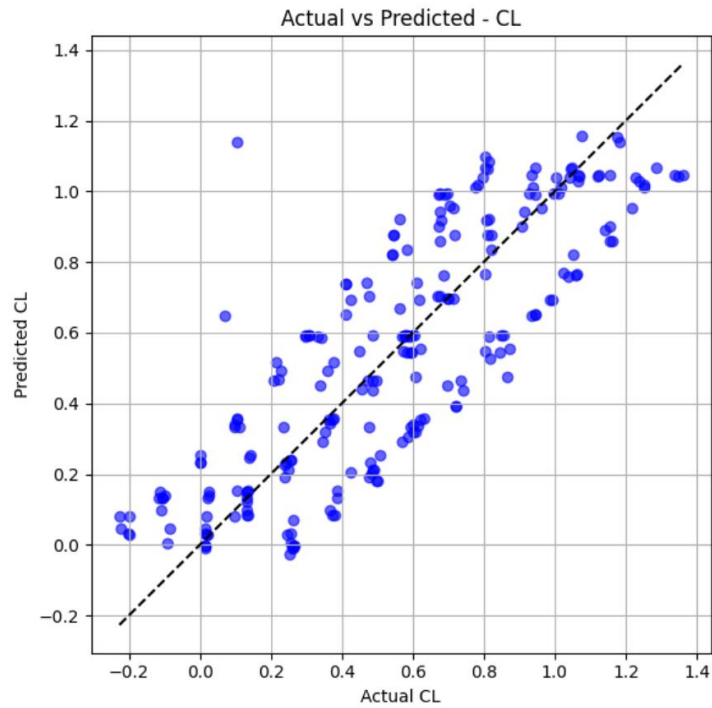


Figure 9. 9 XG-Boost regression for 2D-CL

For 3D Random Forest regressor

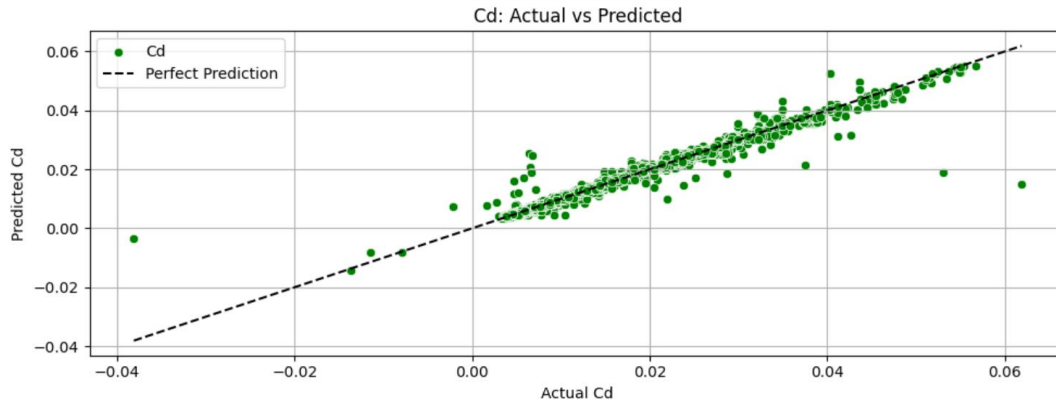


Figure 9. 10 Random Forest for 3D -CD

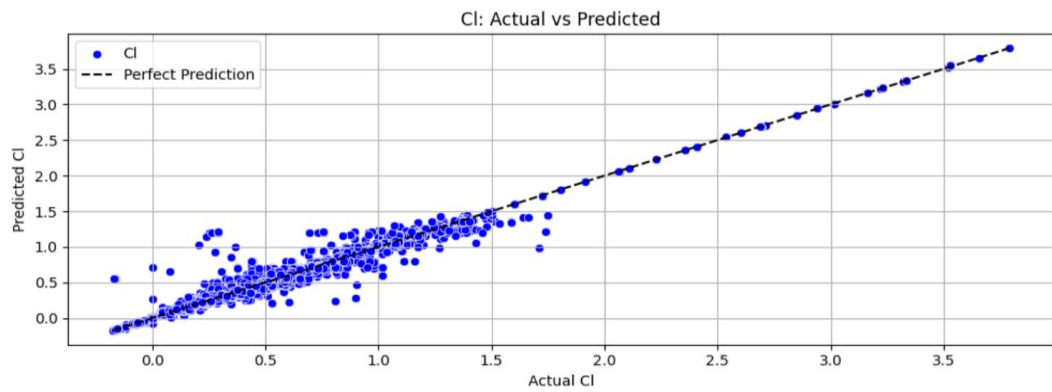


Figure 9. 11 Random Forest 3D Dataset-CL

## 10. User Interface Development

The user interface was designed to provide an interactive, web-based platform for aerodynamic analysis. Its development involved the following components:

### 10.1 Development Environment

- Language: Python
- IDE: Visual Studio Code (VS Code)

## 10.2 Frontend

- Tool: Stream lit library
- Purpose: Provides an interactive web interface for user input and output display.
- Functions:
  - Accepts aerodynamic parameters from the user.
  - Displays results and visualizations (CL, CD, graphs).

## 10.3 Backend

- Tool: Python scripts with scikit-learn integration.
- Purpose: Implements the machine learning models for aerodynamic coefficient prediction.
- Functions:
  - Processes input data from the frontend.
  - Runs the ML prediction engine.
  - Sends results back to the interface for display.

## 10.4 System Architecture

- Data Flow:

User → Stream lit Frontend → Python + scikit-learn Backend → ML Model → Output Visualization
- This structure ensures seamless communication between the machine learning model and the user interface, enabling efficient data input, computation, and visualization.

Following images show us the display of our developed Tool:

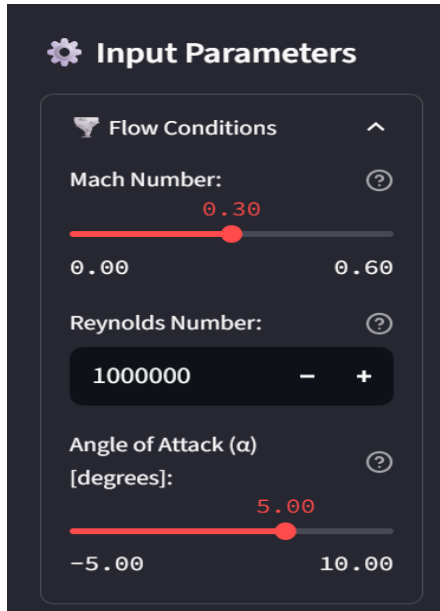


Figure 10. 2 Input parameters in 2D Interface

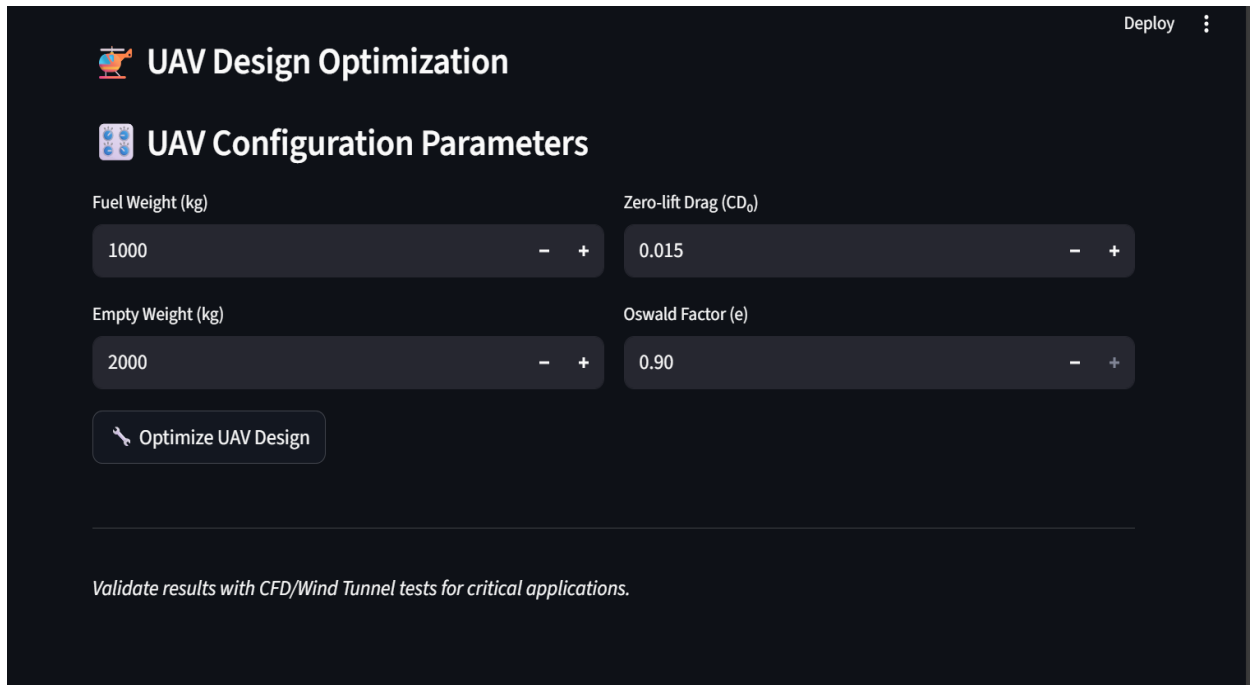


Figure 10. 1 Options of Airfoil in interface



Figure 10. 3 2D Aero Analysis interface with predicted CL and CD

## 10.5 UAV OPTIMIZER SUITE:



The interface for the UAV Design Optimization suite. It features a dark theme with a top bar containing a 'Deploy' button and a menu icon. The main heading is 'UAV Design Optimization' with a drone icon. Below it is the 'UAV Configuration Parameters' section, which includes four input fields: 'Fuel Weight (kg)' set to 1000, 'Zero-lift Drag ( $CD_0$ )' set to 0.015, 'Empty Weight (kg)' set to 2000, and 'Oswald Factor (e)' set to 0.90. Each field has minus and plus buttons for adjustment. A 'Optimize UAV Design' button is located below the inputs. At the bottom, a note states: 'Validate results with CFD/Wind Tunnel tests for critical applications.'

**UAV Design Optimization**

**UAV Configuration Parameters**

Fuel Weight (kg): 1000 - +

Zero-lift Drag ( $CD_0$ ): 0.015 - +

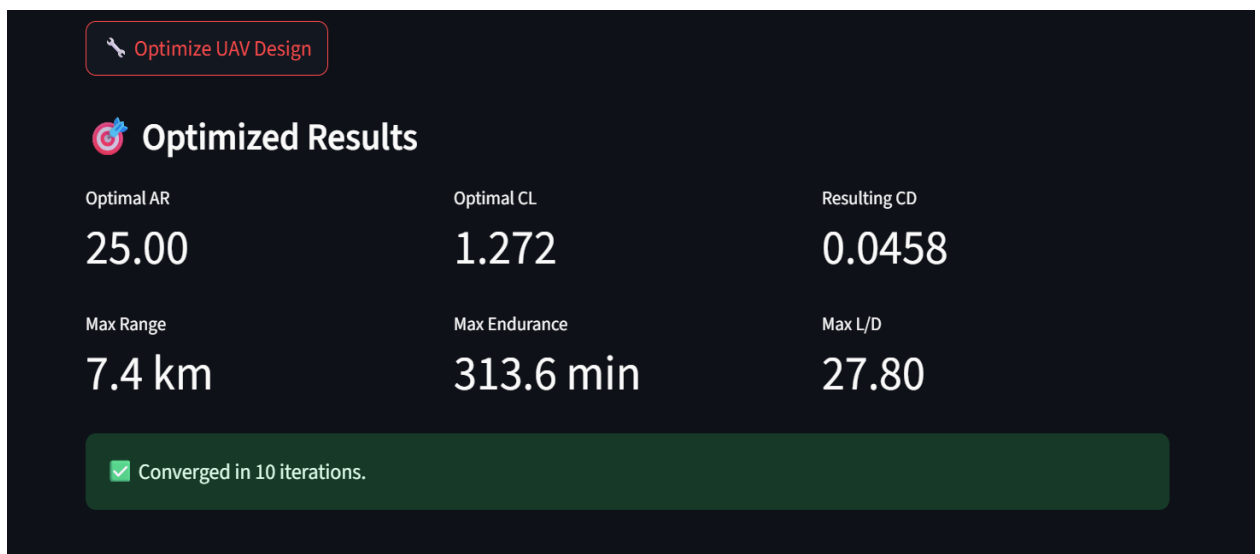
Empty Weight (kg): 2000 - +

Oswald Factor (e): 0.90 - +

[Optimize UAV Design](#)

*Validate results with CFD/Wind Tunnel tests for critical applications.*

Figure 10. 4 Optimizer interface



The 'Optimized Results' section of the interface. It features a red 'Optimize UAV Design' button at the top left. The main heading is 'Optimized Results' with a target icon. Below it is a table of optimized performance parameters. The table has three columns: 'Optimal AR', 'Optimal CL', and 'Resulting CD'. The values are: 25.00, 1.272, and 0.0458 respectively. Below the table, there are three more parameters: 'Max Range' (7.4 km), 'Max Endurance' (313.6 min), and 'Max L/D' (27.80). At the bottom, a green banner indicates 'Converged in 10 iterations.'

[Optimize UAV Design](#)

**Optimized Results**

Optimal AR	Optimal CL	Resulting CD
25.00	1.272	0.0458
Max Range	Max Endurance	Max L/D
7.4 km	313.6 min	27.80

✓ Converged in 10 iterations.

Figure 10. 5 Optimized performance parameters

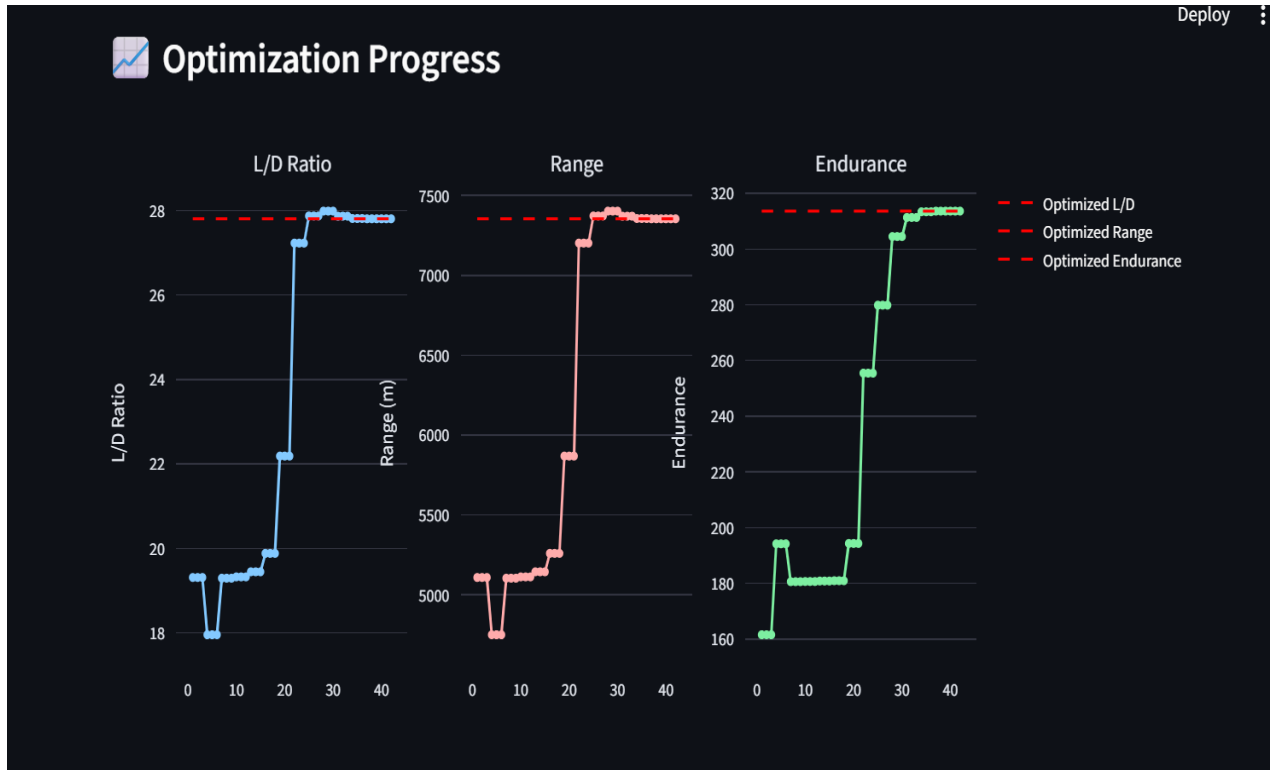


Figure 10. 6 Optimized results in form of graphs

Figure 10.6 shows the input of our optimizer. Our interface receives user inputs like the UAV's gross weight, fuel mass, and  $CD_0$  (zero-lift drag coefficient). The code currently sets the  $CD_0$  value to 0.02 by default, but users can change it if necessary.

The optimizer runs for a predetermined number of iterations after the inputs are supplied, producing graphs that display the outcomes. Using the inputs provided, it maximizes important performance metrics like range, endurance, and lift-to-drag ratio (L/D).

## 10.6 3D Aerodynamic Prediction Tool:

**Input Parameters**

Select Airfoil: NACA 2412 (Index: 0)

☒ Geometric ☐ Flow

Wingspan [m]: 10.00

Mean Aerodynamic Chord (MAC) [m]: 0.100

Taper Ratio: 0.50 (range: 0.40 to 1.00)

**Predict Coefficients**

Figure 10. 8 3D Input parameters

**Input Parameters**

Select Airfoil: NACA 2412 (Index: 0)

☒ Geometric ☐ Flow

Velocity [m/s]: 15.0

Mach Number: 0.044

Angle of Attack (AOA) [degrees]: 0.50 (range: -5.00 to 10.00)

Reynolds Number: 1000000

**Predict Coefficients**

Figure 10. 7 3D interface parameters (flow)

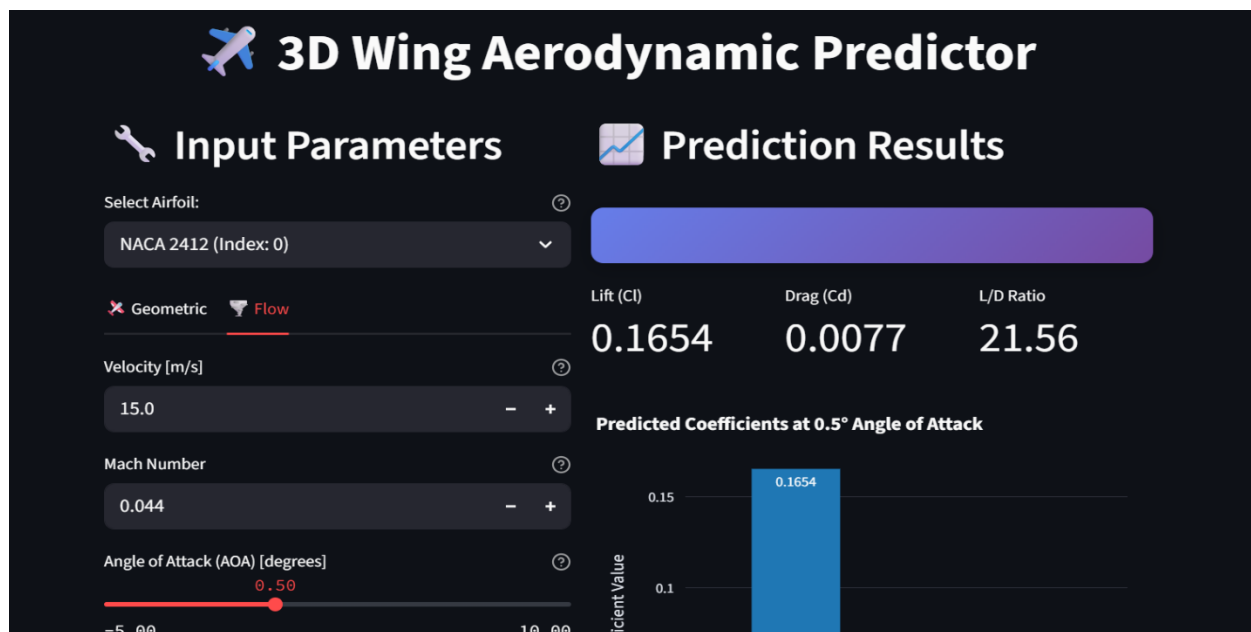


Figure 10. 9 Results display-3D Cl and Cd prediction



### Input Summary

Parameter	Value
Airfoil	NACA 2412
Wingspan	10.00 m
MAC	0.100 m
Taper Ratio	0.50
Velocity	15.0 m/s
AOA	0.5°
Reynolds No.	1,000,000
Mach No.	0.044

Figure 10. 10 Input summery in Interface

Taper ratio, wingspan, angle of attack (AOA), velocity, and airfoil selection for root and tip are among the inputs needed by the 3D interface as shown in figure 10.7 and 10.8.

The system analyzes aerodynamics based on these parameters and outputs the Reynolds number, CL (lift coefficient), and CD (drag coefficient) as shown in figure 10.9. These findings aid in assessing the 3D wing configuration's aerodynamic performance.



## **11. Future Goals and Industrial Relevance**

The developed ML-based aerodynamic prediction tool holds strong potential for industrial adoption and further development. Its future applications and relevance to the UAV industry include:

### **11.1 Rapid UAV Design Prototyping**

The tool can significantly reduce the time and cost required for UAV design iterations by quickly predicting lift and drag values. This capability enables aerospace companies to bring new drone models to market faster, minimizing dependence on lengthy CFD simulations during early design stages.

### **11.2 Integration into UAV Design Software**

The model can be embedded into existing aerospace design platforms, such as XFLR5 or ANSYS add-ons, to provide intelligent suggestions and real-time performance predictions. This integration would allow designers to receive instant aerodynamic insights without the need for complete CFD workflows.

### **11.3 Customized UAV Performance Optimization**

Industries such as defense, agriculture, and delivery services can leverage the tool to fine-tune UAV wings for specific mission profiles—whether the objective is extended range, enhanced endurance, or improved payload capacity—resulting in higher operational efficiency and improved mission success rates.

## 12.Sustainable Development Goals:



*Figure 1 Sustainable Development Goals:*

### 12.1 Goal 9:

Fostering Innovation: The use of machine learning and CFD simulations

represents a significant technological advancement in UAV design and operation, promoting innovation in aerospace technology and autonomous systems.

### 12.2 Goal 12

Responsible Consumption. UAVs optimized for efficiency can replace larger, more energy-consuming vehicles

### 13.References:

- [1]. (PDF) Unmanned Aerial Vehicles: A Review
- [2]. Dronova, C. Kislik, Z. Dinh, and M. Kelly, “A review of unoccupied aerial vehicle use in wetland applications: Emerging opportunities in approach, technology, and data,” *Drones*, vol. 5, no. 2. MDPI AG, Jun. 01, 2021. doi: 10.3390/drones5020045. - Search
- [3]. S. G. Gupta, M. M. Ghonge, and P. M. Jawandhiya, “Review of Unmanned Aircraft System (UAS),” 2013. [Online]. Available: [www.ijarcet.org](http://www.ijarcet.org) - Search
- [4]. A. Koreanschi et al., “Optimization and design of an aircraft’s morphing wing-tip demonstrator for drag reduction at low speeds, Part II - Experimental validation using Infra-Red transition measurement from Wind Tunnel tests,” *Chinese Journal of Aeronautics*, vol. 30, no. 1, pp. 164–174, Feb. 2017, doi: 10.1016/j.cja.2016.12.018. - Search
- [5]. Mardanpour, Pezhman, Mehrabi, and Armin, “C3-FIU05 4. Title and Subtitle 5. Report Date Principal and Considerations for Design of Small Unmanned Aerial Vehicles for Inspection and Survey,” 2019. [Online]. Available: <https://orcid.org/0000-0002-1423-0304> - Search
- [6]. I. Mir, A. Maqsood, and S. Akhtar, “Dynamic Modeling & Stability Analysis of a Generic UAV in Glide Phase,” *MATEC Web of Conferences*, vol. 114, p. 01007, Jan. 2017, doi: 10.1051/matecconf/201711401007. - Search
- [7]. Raymer, D. P. (2018). *Aircraft Design: A Conceptual Approach* (6th ed.). AIAA Education Series. - Search

- [8]. Versteeg, H. K., & Malalasekera, W. (2007). An Introduction to Computational Fluid Dynamics: The Finite Volume Method (2nd ed.). Pearson Education. - Search
- [9]. Bhargava, R., Khurana, H., & Sharma, V. (2021). Machine learning based prediction of aerodynamic coefficients using CFD-generated datasets. Aerospace Science and Technology, 117, 106986. - Search
- [10]. Altug, E., & Kaymaz, I. (2018). CFD-based aerodynamic optimization of fixed-wing UAVs. International Journal of Aerospace Engineering, 2018, Article ID 6842917. <https://doi.org/10.1155/2018/6842917> - Search
- [11]. Zhang, Y., Li, Z., & Zhao, X. (2020). Aerodynamic performance analysis of NACA airfoils for UAV surveillance missions. Aerospace Science and Technology, 104, 105983. - Search
- [12]. Bhargava, R., Khurana, H., & Sharma, V. (2021). Machine learning-based prediction of aerodynamic coefficients using CFD datasets. Aerospace Science and Technology, 117, 106986. - Search
- [13]. Liu, Y., Wang, J., & Chen, L. (2022). CNN-based prediction of airfoil pressure distribution in subsonic flows. Journal of Fluids and Structures, 112, 103532. - Search